DESIGN AND FABRICATION OF METAL-POLYMER BASED CORE-SHELL ARTIFICIAL NANODIELECTRICS FOR CAPACITOR APPLICATIONS

A Thesis

Presented to

the Faculty of the Department of Electrical and Computer Engineering

University of Houston

In Partial Fulfillment

of the Requirements for the Degree of

Master of Science

in Electrical Engineering

by

Deepak Musuwathi Ekanath

May 2012

ACKNOWLEDGEMENTS

I dedicate this work to my father, who has been a role model, encouraged me to face challenges and supported me throughout my life. I thank my family for their support and love throughout my Masters.

I sincerely express my gratitude to Dr. Abdelhak Bensaoula, for giving me an opportunity to work with him for my Master's thesis. His profound knowledge and insights, dedication to research, enthusiasm for work, have been and will continue to be a great source of inspiration for me.

I would like to thank Dr. David Starikov and Dr. Len Trombetta for accepting my invitation to serve on my thesis committee. I would like to thank Dr. Nacer Badi for his constant guidance and support. I thank Dr. Raghu Singh for his assistance and help during the processing and helping me with chemistry related issues. I extend my gratitude to Mr. Rajesh Bikky for his help and training on the instruments and simulation software.

A special thanks to Dr. Rajeev Pillai who has been a constant source of inspiration and fostering me to learn the core concepts of device fabrication and processing. I would also like to thank the entire nitride group members and the INE group members for their direct and indirect support on this project.

DESIGN AND FABRICATION OF METAL-POLYMER BASED CORE-SHELL ARTIFICIAL NANODIELECTRICS FOR CAPACITOR APPLICATIONS

An Abstract

of a thesis

Presented to

the Faculty of the Department of Electrical and Computer Engineering

University of Houston

In Partial Fulfillment

of the Requirements for the Degree of

Master of Science

in Electrical Engineering

by

Deepak Musuwathi Ekanath

May 2012

ABSTRACT

The need for high storage capacitors led to the development of polymer based capacitors. The permittivity of the polymer as well as its dielectric strength can be tuned to desired characteristics by introducing either ceramic or metal nano fillers. Usage of ceramic fillers would need higher loading, leading to less flexibility and compatibility with printed circuit boards. Thus metal nano fillers can be used effectively to enhance the dielectric properties.

My thesis work involves loading of Silver (Ag) and Ag@SiO_2 nano particles by dispersing them in a Polyvinyl Pyrrolidone (PVP) matrix. This nano composite solution acts as a dielectric for a parallel plate polymer capacitor. The capacitance and the thickness of the film were measured in order to determine the K value of the dielectric. The capacitor parameters such as the dissipation factor and breakdown voltages were also determined. The dielectric constant of PVP increased from 7 to 40 at 0.08% loading of silver nano particles. Effective medium theories and percolation theories were implemented to analyze the theoretical value of effective dielectric constant. Finite Element Method based simulations were used to study the electric field and polarization patterns inside the dielectric.

TABLE OF CONTENTS

LIST OF FIGURES

LIST OF TABLES

CHAPTER 1. INTRODUCTION

1.1 Energy Storage

The process of storing any form of energy by using devices or any other physical media that can be retrieved at any point of a future timefalls under the energy storage category. Storing energy allows one to balance the supply and demand for energy, thus directly affecting the economic development of the nation.

"Energy can neither be created, nor be destroyed. It can only be converted from one form to another without any loss."- states the conservation of energy law.

Technological advances have led to the development of various types of energy conversion methodologies from any initial source into electrical energy. Electrical energy can now be obtained from various forms of mechanical energy, such as wind energy, hydraulic energy, as well as bio-chemical, radiation and atomic energy. With an increase in productivity, the demand for storing energy has also increased. In particular, there is an increase in demand for devices that can store a large amount of charge and deliver it instantaneously [1-3].

Modern electronic boards are comprised of ~40% of passive devices [1,2]. The passive devices include capacitors, resistors, inductors, etc. These devices are used for charge storage, and for controlling current-voltage phase angle and impedance in the circuit. Traditionally batteries are implemented for charge storage. Future technologies would demand high performance with miniature circuits. Hence embedded passives may be a very good option for charge storage in micro level circuits.

1.2 Organization of thesis

This thesis contains seven chapters namely the Introduction, Literature review, Background theory, FEM Simulation, Experimental procedure, Results and future work and conclusion.

The first chapter gives an introduction to the project and defines the problem statement. The second chapter deals with the different types of commercial capacitors and advanced capacitors like high temperature capacitors, High K-value capacitors and High voltage withstanding capacitors. The third chapter describes the background theory which helps in understanding the working of the nano dielectrics. The different equations that will be applied for theoretical calculations are also dealt in the same chapter. The fourth chapter introduces the concept of Finite Element Analysis, which is the base for building models to be used for COMSOL Multipyhysics software. It describes the steps and settings to build the entire model and to obtain the results out of them. The fifth chapter explains the experimental procedure performed for fabrication and characterization of the nano dielectric capacitor and the equipment used for the same. The sixth chapter illuminates the results obtained using a different approach and lists out the directives for future work. The thesis is concluded in the seventh chapter by the summary of outcomes, which is followed by the list of references.

1.3 Embedded passives

Embedded passives are passive components placed between the interconnecting wires of a printed wiring board. Implementation of embedded passives would free up surface real estate allowing either a smaller footprint or more devices to be placed on the same size substrate, thereby enormously increasing the function potential of small electronic devices. Figure 1.1 shows the cross sectional view of a printed circuit board containing the embedded passive devices.

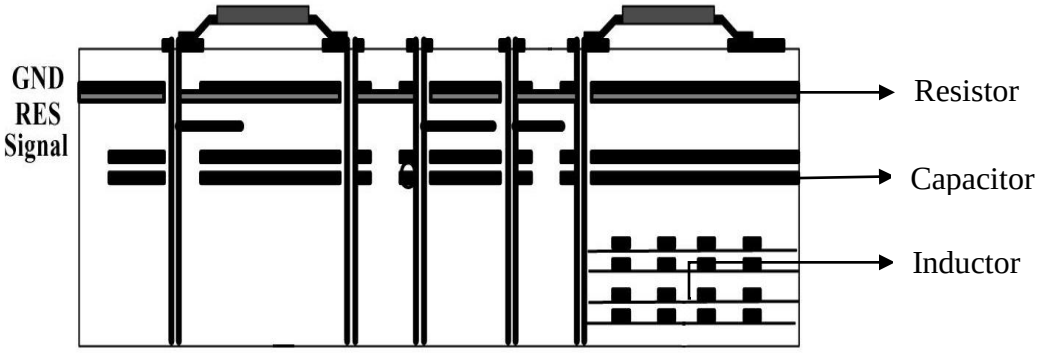

Figure 1.1. Cross sectional view of a printed circuit board with embedded passives

There are many other potential advantages to embedding passives in printed wiring boards for many types of applications. Capacitors could be placed directly underneath the active component support, thereby reducing the number of layers and interconnecting vias. This would simplify board construction thereby, reducing costs and lower parasitic inductance and cross talk.

1.4 Capacitors

A capacitor is basically a combination of two parallel metal plates with a dielectric in between them. A dielectric can be considered as a quasi-conductor. A capacitor can be designed for AC and also DC applications. In October 1745, Edwald Georg von Kleist, a German scientist found that charge could be stored by connecting a high-voltage electrostatic generator by a wire to a volume of water in a hand-held glass jar [42]. Von Kleist's hand and the water acted as conductors and the jar as a dielectric. Von Kleist found, after removing the generator, that touching wire resulted in a painful spark. This was the base for the capacitor working and following year, a Dutch physicist Pieter van Musschenbroek invented a similar capacitor, which was named as the Leyden jar. Later in the 20^{th} century, when technology demanded more flexible capacitors, that can work at high frequencies with low inductance, a flexible dielectric sheet such as oil paper was sandwiched between metal sheets, thus leading to modern capacitors.

When an electric field is applied between the metal plates, with a dielectric in between them, the charge doesn't flow through the material. Instead, the positive charges are aligned towards the direction of the applied electric field, thus leading to storage of charges at the metal plates. This is termed as dielectric polarization.

The capacitance of a capacitor greatly depends on the polarizability of the dielectric. With increase in polarization, generated electric field increases. Thus the charge storage capacity of the capacitor also increases. A cross section of a simple capacitor is drawn as shown in figure 1.2.

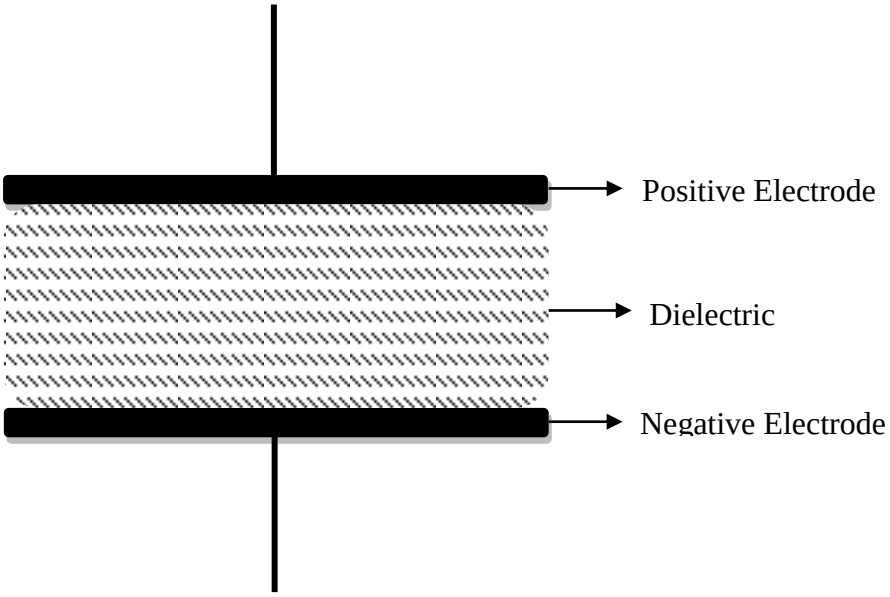

Figure 1.2. Cross section of a parallel plate capacitor

1.5 Capacitance Improvement

The capacitance of a capacitor determines the quantity of charge it can store. Its unit is Farad. One Farad is one Coulomb of charge applied per one Volt. The capacitance of a capacitor is given by the equation,

$$C = \frac{\varepsilon_0 \varepsilon_r A}{d}, \tag{1}$$

where A is the area of the metal plates, εo is the permittivity of free space with value 8.854x10-4, εr is the relative permittivity, which can also be denoted by K and d is the distance between the metal plates.

Thus from the equation, in order to increase the capacitance, three strategies can be adopted:

1. Increasing the area of the metal plates
2. Decreasing the distance between the plates
3. Increasing the dielectric constant

1.5.1 Increasing the area of plates

As the area of the metal plate increases, the capacitance value also increases. This can be achieved only up to a small value. As we increase the area more and more, the capacitor becomes more bulky and it would be difficult to include the capacitor in miniature level circuits. This would make the capacitor less flexible too. Hence increasing the area of the metal plates is not a very good option.

1.5.2 Decreasing the distance between the plates

The distance of separation is inversely proportional to the capacitance. Hence decreasing the distance may seem to be a good idea to increase the capacitance. But as the distance between the plates decreases, the charges can be easily attracted towards each other thus creating an electrical short. Hence it no longer acts as a capacitor, but just a shorted wire. This is also termed as dielectric breakdown. Hence capacitors with very low distance of separation may have very low dielectric breakdown strength.

1.5.3 Increasing the dielectric constant

Increasing the dielectric constant (K) has been a promising technique in increasing the capacitance of the capacitor. Increasing the K value wouldn't degrade the performance of the capacitor. Thus choosing a dielectric with high K value would be a good approach.

1.6 Aim of the project

The outlook of the project is the fabrication of nanodielectric capacitors for both embedded and discrete capacitor applications. The primary focus is to increase the effective dielectric constant of the composite formed by embedding metal-silica and metal- polymer based core-shell nanoparticles in a Polyvinyl Pyrrolidone host matrix. Capacitors fabricated by using such composites were tested and characterized.

Advances in computer technology have made accessible powerful design and simulation tools for complex structures like nanodielectrics. Finite element method (FEM)-based COMSOL Multiphysics software is used in this work to simulate the electrical properties of nanocomposites. Dielectric constant of the composite is calculated for different loadings of Silver nano particles in a PVP and PS matrix for 2D and 3D models. Effective medium theories are used to calculate the effective dielectric constant of the composite. Percolation theory is used to calculate the effective dielectric constant of the composite for different loadings of the nanoparticles[4].

CHAPTER 2. LITERATURE REVIEW

2.1 Capacitors

2.1.1 Mica capacitors

Mica is one of the oldest dielectric materials used in capacitors, with dielectric constants in the range of 5-7; it is electrically, chemically, and mechanically stable and is ranked high in quality factor and breakdown voltage. When combined with low inductance designs, mica capacitors are useful for high-frequency and RF applications [6]. Mica capacitors, however, are bulky because of their low dielectric constant, which led to their decline and paved the way for the popularity of ceramic capacitors.

2.1.2 Ceramic Capacitors

Ceramic capacitors, made of ceramic materials, are the most widely used capacitors because of their robustness, cost and efficiency. Ceramic capacitors are made from a variety of materials that come in many forms. The most commonly used materials are titanium dioxide, strontium titanate, and barium titanate [7]. The Electronic Industries Alliance (EIA) categorizes ceramic capacitors into three classes: Class-1 capacitors are usually made from magnesium titanate or calcium titanate. In terms of operational temperature, the Class-1 capacitors are the most stable of all ceramic capacitors. Class-2 capacitors are less stable than Class-1, but are more efficient volumetrically. Class-2 capacitors are used as decoupling, by-pass, and coupling capacitors because less efficiency is not an issue in these applications. Class-3 capacitors have high volumetric efficiency and high dielectric constant at room temperature. Barium titanate, with a dielectric constant of up to 1250, is the dielectric material used in class-3 capacitors [7].

Class-3 capacitors have low accuracy and stability and cannot withstand high voltages. Some applications for these capacitors include use as decoupling capacitors and other power supply applications.

2.1.3 Electrolytic capacitors

Aluminum and tantalum capacitors are electrolytic capacitors. An ionic liquid electrolyte is used as one of the terminals in the electrolyte capacitors, and a thin layer of metal oxide is used as the dielectric. Electrolytic capacitors have high volume efficiency and stability at room temperature but their drawbacks limit their application. The voltage applied to these capacitors must always be polarized; one terminal must always be at a positive voltage, the other at a negative. They have low breakdown voltage, high leakage current and shorter life span compared to the other types of capacitors.

2.1.4 Glass capacitors

Glass capacitors offer the best performance and reliability in the capacitor industry. Their dielectric material is glass enclosed in a metal casing with alternate layers of glass and electrode material sealed precisely to form a monolithic block. Glass capacitors have low dielectric loss, fixed temperature coefficient, extended life, and zero piezoelectric noise [8,9]. Stable performance and excellent frequency response make them an obvious choice for high-end applications like aerospace and the military, but they are usually bulkier and more expensive.

2.1.5 Polymer Film Capacitors

Polymer film capacitors have been in use for more than 50 years. They're attractive to engineers and scientists researching pyroelectric and embedded capacitor applications, electromechanical transducers, and microwave communication devices [10].

Table 2.1: General characteristics of a few dielectric films

Plastic Film	**Dielectric Constant**	**Maximum Temperature [^{0}C]**	**Breakdown Voltage [V/µm]**	**Dissipation Factor % 1kHz**	**Energy Density (J/cc)**
Polypropylene(PP)	2.2	105	640	<0.02	1-1.2
Polyester(PET)	3.3	125	570	<0.5	1-1.5
Polycarbonate(PC)	2.8	125	528	<0.15	0.5-1
Polyvinylidene-fluoride(PVDF)	12	125	590	<1.8	2.4
Polyethylene-naphlate(PEN)	3.2	125	550	<0.15	1-1.5
Polyphenylene-sulfide(PPS)	3.0	200	550	<0.03	1-1.5

Polymer film capacitors have a low glass transition temperature, so they are not preferred for applications where temperature exceeds 200^{0}C. Table 2.1 shows the main features of some commonly used polymer dielectric films [11].

2.2 Research on capacitors

2.2.1 High temperature capacitors

(a) Ceramic Capacitors

Capacitors using a ceramic dielectric medium have been found to be useful at high temperatures. Ceramic multilayer capacitors have been shown to function up to 200^{o}C for approximately 1000 hours [13]. However the disadvantage of using ceramic dielectrics is that at high temperatures, the K value of the capacitor goes down. Figure 2.1 shows the temperature variation of a ceramic capacitor with a medium-K dielectric [14].

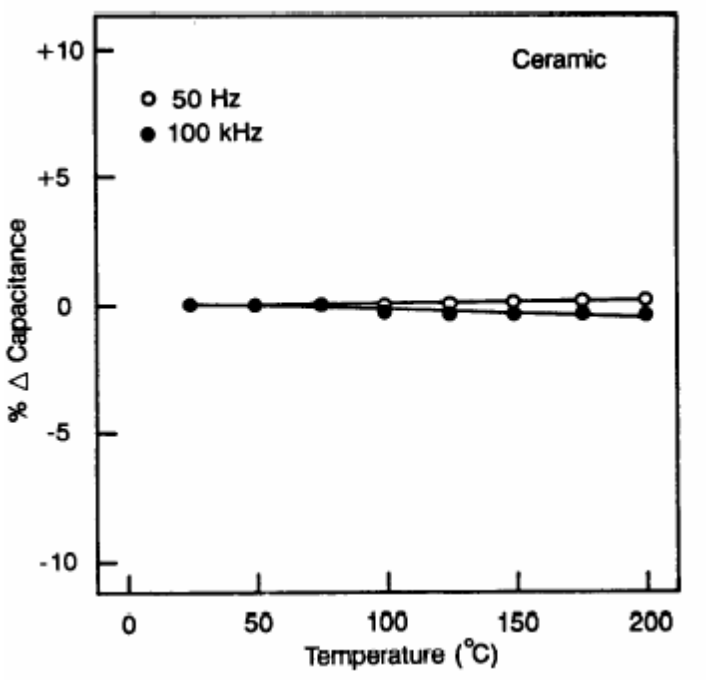

Figure 2.1. Change in capacitance of a ceramic capacitor with temperature

The advantage of using ceramic capacitors is that there is no pull-away in their epoxy coating. They are resistant to moisture penetration and provide supreme volumetric efficiency. They have a wide variety of applications ranging from Military and aerospace to electric ballast applications.

(b) Glass capacitors

Glass dielectric capacitors have been found to be well suited for high temperature applications as they can withstand more than 300 ^{o}C. In fact, these dielectrics are commonplace in capacitors for circuits where low noise, high stability and high Q are important [15]. They can withstand harsh environments and have minimal aging effects, with low loss and zero piezoelectricity effects. A major negative characteristic of glass-based capacitors is the low volume efficiency and sharp drop in capacitance with increasing temperature. The drop in capacitance at high temperatures is more in this case, than that of the ceramic capacitors. Hammoud et al [14] addressed this property in their work on glass capacitors as shown in figure 2.2.

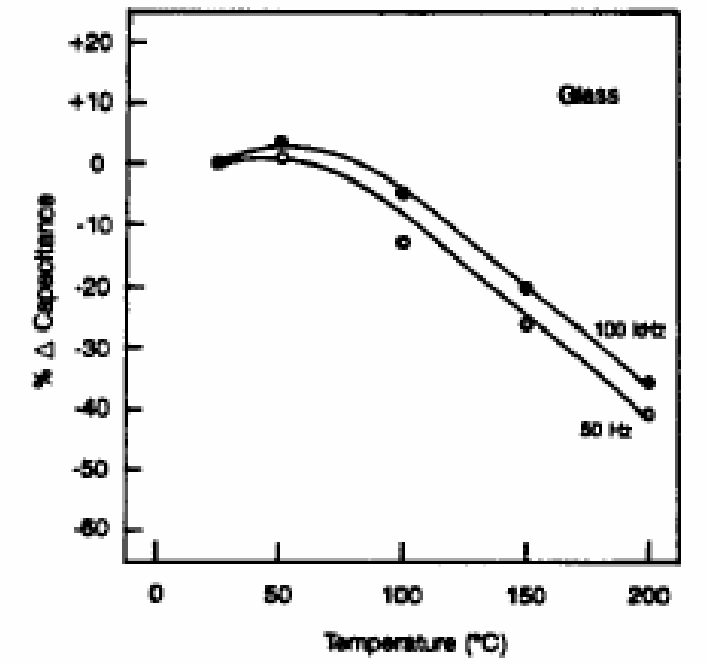

Figure 2.2. Change in capacitance of a glass capacitor with temperature

2.2.2 High voltage capacitors

(a) Electroltic capacitors

Electrolytic capacitors are capacitors in which one or both of the plates is a non-metallic conductive substance, an electrolyte. Electrolytes have lower conductivity than metals, so are only used in capacitors when metallic plate is not practical. Most common cases include, when the dielectric surface is fragile or rough in shape or when ionic current is required to maintain the dielectric integrity. The dielectric material of electrolytic capacitors is produced from the metal form by using an anodizing process. During this process, current flows from the metal anode-which must be a valve metal such as aluminum, niobium, tantalum, titanium or silicon, through a conductive bath or special forming electrolyte to the cathode. The flow of current causes an insulating metal oxide to grow out of and into the surface of the anode [16].

The thickness, structure and composition of this insulating layer determine its dielectric strength. The applied potential between the anode metal and the bath cathode must be above the electrolyte breakdown voltage before significant current will flow and below the oxide breakdown voltage to prevent shorting.

2.2.3 High K capacitors

(a) Ferroelectric Ceramic/Polymer Composite Capacitors

In ceramic/polymer composites, traditional ceramics such as $BaTiO_3$, $BaSrTiO_3$, and $PbZrTiO_3$, are modeled as fillers in a polymer matrix [17, 18]. These composites display relatively low *K* values of less than 100, with additional disadvantages such as low adhesion strength, and poor processability [1]. The *K* values of these composites

were successfully increased, however, to 200 by modifying the intrinsic *K* of the bare polymer. A concern with ceramic/polymer composites is the high ceramic loading, which results in technical barriers such as poor dispersion of filler and low flexibility.

(b) Conductive Filler/Polymer Composite Capacitors

Conductive filler/polymer composites, designed by using principles based on percolation theory, are an alternate approach to ceramic/polymer composites. Conductive filler/polymer composites are advantageous because they require a smaller fraction of filler volume. The filler sizes used in these types of composites are typically in the range of a few microns [20]. Higher *K* values can be predicted with conductive filler/polymer composites when the volume fractions of fillers reach the vicinity of the percolation threshold [20]. In these kinds of composites, high *K* values are accompanied by a high-loss tangent due to the presence of metal fillers.

(c) All-Organic Polymer Composite Capacitors

Organic fillers with high *K* values are dispersed in a polymer matrix to form all-organic polymer composites. The dielectric loss of these composites is much lower, while the maintained *K* value is much higher, than for previously mentioned composites. The fillers are chemically modified by attaching highly reactive functional-radical groups, thereby increasing compatibility between polymer and fillers. This chemical modification led to a further increase in the *K* value, and the loss tangent remained low [21].

(d) Nanocomposite capacitors

Nanoparticles exhibit interesting physical, chemical, electrical, and magnetic properties [22]. Because of these unusual properties, a lot of research has been carried out on nanomaterials as fillers for nanocomposites. Nanofillers/polymer composites make a good choice for embedded capacitors because they possess advantages of both polymers and nanoparticles. Another advantage of nanocomposites is their ability to attain higher capacitance densities in thinner films. Because of the formation of clusters of nanoparticles, a conducting path in the dielectric can be formed, which may result in a catastrophic failure of the device. A uniform dispersion of nanoparticles, therefore, is necessary for improved dielectric properties and reproducibility.

(e) Core-shell hybrid filler polymer composite capacitors

Direct contact of the conductive fillers will result in a high dielectric loss, which might also lead to the formation of a conductive path in the polymer composites. A core-shell structure in which an insulating shell is coated around each conducting filler particle, is proposed for the nanofillers. The non-conductive shells act as inter-particle barriers and prevent the conductive cores from coming into contact with each other. Core/shell structured nanoparticles can be synthesized using methods such as the sol-gel process of coating a non-conductive shell around each core or oxidizing a conductive core to form a shell of its non-conductive oxide, etc. [23]. Core-shell filler/polymer composites have a high K value because of an increase in the net polarization of the dielectric and low loss tangents of the non-conductive shell.

CHAPTER 3. BACKGROUND THEORY

3.1 Factors affecting capacitor performance

3.1.1 Dielectric constant

Every material has its own dielectric constant, with a value greater-than or equal-to one. Vacuum has the smallest dielectric constant value of one. The dielectric constant (*K*), also known as relative permittivity (ε_r), is a dimensionless quantity and is defined as the ratio of permittivity of the material (ε) to permittivity of vacuum (ε_0). A capacitor filled with an insulating dielectric material can store *K* times more charge than an air dielectric capacitor with the same dimensions. This implies that, as *K* value increases, *C* also increases. Dielectrics with high *K* values, therefore, are desired in the design of high-storage capacitors. For every material with no dielectric loss, *K* is a single constant value, but in reality, every material has some dielectric loss associated with it. Under an alternating electric field, the dielectric constant can be expressed by a complex permittivity as

$$\varepsilon^* = \varepsilon^{'} - j\varepsilon^{"} = \varepsilon_0\varepsilon_r - j\varepsilon^{"} \quad (2)$$

or

$$\varepsilon^* = |\varepsilon|e^{-j\delta}, \quad (3)$$

where ε' is the real permittivity, ε'' is the imaginary permittivity, and δ is the dielectric loss angle (Equation 4) [24]. Real permittivity, ε', is directly related to the *K* of a material, and ε'' is the dielectric loss factor of the material. The magnitude and phase notation of Equation 2 is represented by Equation 3, and is rarely used.

3.1.2 Dielectric loss

Dielectric loss in capacitors is a measure of its energy loss. This is due to the motion of mobile charges inside the dielectric under the influence of an alternating current. Due to the dielectric loss, the current to voltage angle deviates from an ideal value of 90^0. This angular difference is termed as loss angle.

Dielectric loss is usually expressed as the dissipation factor (*D*). A dissipation factor under 0.1 percent is considered low and 5 percent is high [8]. The equation for the dissipation factor is

$$\tan \delta = \frac{\varepsilon''}{\varepsilon'}. \tag{4}$$

A quality factor (*Q*) is another parameter used to represent the quality of the dielectric, which is the reciprocal of a dissipation factor. A very high quality factor is usually desired for a good capacitor. The equation for a quality factor is represented as

$$Q = \frac{1}{\tan \delta}. \tag{5}$$

The total amount of energy dissipated by the dielectric is given by energy loss (*W*). Energy loss is directly proportional to dielectric loss, and is shown as

$$W = \pi \varepsilon' \xi^2 f \tan \delta, \tag{6}$$

where ξ is the applied electric field strength and *f* is the frequency.

3.1.3 Dielectric strength

Dielectric strength or dielectric breakdown is a measure of the maximum electric field that a capacitor can withstand without facing a catastrophic breakdown. Breakdown voltage is the maximum voltage that a material can withstand before losing its insulating properties. At any voltage higher than the breakdown voltage, the device can no longer

function as a capacitor, and the damage is usually permanent, with the exception of gas dielectrics [25]. Unlike solid dielectrics, the dielectric strength of gas dielectrics is recovered once the current flow is externally interrupted.

3.1.4 Polarization

The amount of charge stored by a material is directly related to its dielectric polarization. An electric field induces electrical dipoles in the dielectric medium and aligns them according to the direction of the field. There is a slight change, therefore, in the position of positive and negative charge clouds under the influence of an electric field; this effect is known as dielectric polarization.

There are different types of dielectric polarizations, namely electronic polarization P_e, ionic polarization P_i, molecular polarization $P_{m,}$ and space charge polarization P_s. The total polarization is a sum of individual components, written as

$$P = P_e + P_i + P_m + P_s. \tag{7}$$

Electronic polarization (P_e) occurs in neutral atoms and is usually very small as compared to the other forms of polarization. Electronic polarization can react to very high frequencies, up to the order of 10^{15} Hz. Ionic polarization (P_i) involves the movement of ionic species in the presence of an electric field. This type of polarization is most prevalent at low frequencies and can result in a very high value of K and losses in the system. Molecular or dipole polarization (P_m) is present in materials with permanent dipoles created by the unbalanced distribution of the cloud charge, which can react to frequencies in the range of 10^{11} to 10^{12} Hz. Space charge (P_s) occurs in heterogeneous systems, such as composites, where there is a significant difference in the properties of

the constituent materials. There is a charge build-up at the interface of the constituents that leads to an interfacial polarization (P_s). The frequency range of P_s is 10^{-3} to 10^{3} Hz.

3.2 Drude theory of dielectric function

The dielectric function of any material consists of a real term (ε') and an imaginary term (ε''). The real term (ε') determines the polarizability of a material in the presence of an electric field, and ε'' determines its intrinsic loss mechanisms [30]. For noble metals such as Silver, the complex dielectric function can be decomposed into two components [26-29]. The first component is the Drude free-electron term, and the second component is the substantial contribution of the bound or inter-band electrons. Since the dielectric function is additive, it can be written as the sum of free electron and inter-band electron contributions using

$$\varepsilon_{bulk}(\omega) = \varepsilon_{free}(w) + \varepsilon_{inter}(\omega), \tag{8}$$

where $\varepsilon_{bulk}(\omega)$ is the bulk dielectric function, $\varepsilon_{free}(\omega)$, and $\varepsilon_{inter}(\omega)$ are the free electron and inter-band electron terms of the dielectric functions respectively.

The complex dielectric function of the inter-band electrons is calculated by taking into account the transitions between d-band and conduction sp-band electrons. The imaginary part of the bound-electron dielectric function arises from inter-band transitions, and the real part arises from polarizability of the bound d-band electrons of Silver [29].The expression for dielectric function of bound electrons can be written using the Lorentz oscillator model [26] given by

$$\varepsilon_{inter} = \frac{{\omega_{pb}}^2}{{\omega_0}^2 - \omega^2 - i\omega\gamma_b}, \tag{9}$$

where ω_{pb} is the plasma frequency, ω_0 is the bound-electron resonant frequency, $1/\gamma_b = T_b$ is the bound-electron decay time, $\omega=2\Pi f$ is the angular frequency, and f is the frequency. According to Drude model [26, 27], the complex dielectric function for free electrons is

$$\varepsilon_{free} = 1 - \frac{{\omega_{pf}}^2}{\omega^2 + i\omega\gamma_0}, \tag{10}$$

where ω_{pf} is the plasma frequency, and $1/\gamma_0 = T_0$ is the free-electron scattering time. Table 3.1 shows the values of all parameters used to calculate $\varepsilon_{bulk}(\omega)$ and their references.

Table 3.1: Parameters involved in calculation of the dielectric function of Silver

Parameter	**Parameter Symbol**	**Value**	**Reference**
Plasma Frequency	ω_{pf}, ω_{pb}	$2.17*10^{15}$ Hz	Taken from COMSOL
Bound electron damping term	γ_b	$1.088*10^{14}$ Hz	"
Resonant frequency	ω_0	$7*10^{15}$ Hz	"
Free electron damping term	γ_0	$0.3*10^{14}$ Hz	"
Fermi velocity	V_f	$1.38*10^{6}$ m/s	"

The bulk dielectric constant of Silver is written as

$$\varepsilon_{bulk}(\omega) = 1 - \frac{{\omega_{pf}}^2}{\omega^2 + i\omega\gamma_0} + \frac{{\omega_{pb}}^2}{{\omega_0}^2 - \omega^2 - i\omega\gamma_b}. \tag{11}$$

At room temperature, the electron mean free path of Silver is 40nm and 39nm for copper [31]. For metal particles smaller than the electron mean free path, decay time is particle-size dependent [26], which is given by

$$\gamma_f = \frac{1}{T_f} = \frac{1}{T_0} + 2\frac{V_f}{d}, \tag{12}$$

where T_0 is the scattering time of the bulk material, V_f is the Fermi velocity, and d is the diameter of the particle. Through this modification, size dependencies of the Silver particles are easily incorporated into its dielectric function expression [29] which can be written as

$$\varepsilon(d,\omega) = \varepsilon_{bulk}(\omega) + \frac{{\omega_{pf}}^2}{\omega^2 + i\omega\gamma_0} - \frac{{\omega_{pf}}^2}{\omega^2 + i\omega\gamma_f} \tag{13}$$

and

$$\varepsilon(d,\omega) = 1 - \frac{{\omega_{pf}}^2}{\omega^2 + i\omega\gamma_f} + \frac{{\omega_{pb}}^2}{{\omega_0}^2 - \omega^2 - i\omega\gamma_b}, \tag{14}$$

where $\varepsilon(d,\omega)$ is the size-dependent dielectric constant of a noble metal.

3.3 Effective medium theory

Effective medium theories (EMTs) are used to calculate effective properties of a medium with inclusions. EMTs and other mean-field like theories are physical models based on the properties of individual components and their fractions in the composite [32, 33]. Dielectric constant and conductivity are the properties usually calculated with EMTs. There are many EMTs, and each theory tends to be accurate at different conditions. The most popular of the EMTs [32, 34] are the Maxwell model

$$\varepsilon_{eff} = \varepsilon_h + 3f\frac{\varepsilon_i - \varepsilon_h}{\varepsilon_i + 2\varepsilon_h}\varepsilon_h, \quad (16)$$

Maxwell – Garnett model

$$\varepsilon_{eff} = \varepsilon_h\left[\frac{1 + 2f\left(\frac{\varepsilon_i - \varepsilon_h}{\varepsilon_i + 2\varepsilon_h}\right)}{1 - f\left(\frac{\varepsilon_i - \varepsilon_h}{\varepsilon_i + 2\varepsilon_h}\right)}\right], \quad (17)$$

Symmetric Bruggeman model (also termed as Bottcher)

$$\varepsilon_{eff} = \frac{1}{4}\left[3f(\varepsilon_i - \varepsilon_h) + 2\varepsilon_h - \varepsilon_i + \sqrt{(1-3f)^2\varepsilon_i{}^2 + 2(2 + 9f - 9f^2)\varepsilon_i\varepsilon_h + (3f-2)^2\varepsilon_h{}^2}\right], \quad (18)$$

Asymmetric Bruggeman model

$$\frac{\varepsilon_i - \varepsilon_{eff}}{\varepsilon_i - \varepsilon_h} = (1-f)\left(\frac{\varepsilon_{eff}}{\varepsilon_h}\right)^{\frac{1}{A}}, \quad (19)$$

and Looyenga model

$$\varepsilon_{eff} = \left[\left(\varepsilon_i{}^{\frac{1}{A}} - \varepsilon_h{}^{\frac{1}{A}}\right)f + \varepsilon_h{}^{\frac{1}{A}}\right]^{A}, \quad (20)$$

where ε_{eff} is the effective dielectric constant of the medium, f is the volume fraction of the filler, ε_i is the dielectric constant of the core-shell filler, ε_h is the dielectric constant of the host polymer matrix, and A is a depolarization factor, which depends on the shape of inclusions. The value of A is two for disk fillers and three for spherical fillers.

3.4 Percolation theory

Percolation was originally studied as a mathematical subject, but its broadest applications are found in the field of materials research [35]. Percolation theory takes into account the distribution of a minor phase in the microstructure of the composite, which

depends on its shape, size, and orientation. Percolation theory is one of the easiest mechanisms to model disordered systems because it has little statistical dependency; percolation is an easy concept to realize even for the most complex systems, and its outcomes are realistic for qualitative predictions of random composites [36]. Percolation theory is significant when loading of a minor phase of composite (fillers) reaches a critical value; at this critical value, substantial changes take place in the physical and electrical properties of the system, sometimes on the order of more than a hundred times. This critical fraction of filler is called the percolation threshold, f_c. The abrupt changes in the properties of the system are particularly predominant if the components of the composite have large differences in their properties. Ag filler and the PS matrix, discussed in this work, have varying electrical properties. Ag has high conductivity of $63*10^6$ S-m^{-1} , while PS has low conductivity of $1*10^{-16}$ S-m^{-1}.

A simple power law describes the significant changes in properties of the system near the percolation threshold [35],

$$\frac{K}{K_h} = |f - f_c|^{-s}, \tag{21}$$

where K is the dielectric constant of the composite, K_h is the dielectric constant of the matrix (PVP), f_c is the percolation threshold, f is the filler volume fraction, and s is an exponent of a value of about one.

3.5 Finite element method

Finite element method (FEM), often known as finite element analysis (FEA), is a numerical technique used to find approximate solutions of partial differential and integral equations of engineering and physics problems [37, 38]. FEM requires a problem to be

defined in geometry and subdivided into a number of symmetrical identities, called mesh elements. The modeling of complex engineering systems involves designing, simulating, analyzing, post-processing, testing and fabricating [39]. Modeling and simulating techniques prove to be cost effective by prototyping and testing a product before it is actually manufactured. Computational modeling usually involves four major steps:

- Drawing the geometry
- Meshing (discretization)
- Setting material properties
- Specifying physical (domain), boundary, and initial conditions.

Complex structures require great effort to draw an accurate representation of the original geometry; significant progress in CAD tools has increased the ease and accuracy of this kind of drawing. Meshing divides the geometry into small, discrete identities called elements, or cells [39]. Unknown variables are approximated from known functions through the process of meshing, which applies to the small cells rather than to the entire geometry. Individual solutions from all the cells are integrated and approximated to get a solution for the entire geometry.

Materials used for various engineering applications are chosen because of their unique properties, yet it is important to consider the properties of materials in any simulation, as they can alter the output in many ways. In addition to the properties of materials, the initial, boundary, and domain conditions also play a role in the simulation. The four major modeling steps are performed, and the defined problem is simulated to obtain results; post-processing assists in analysis of the results. Simulation is an iterative process, repeated until desired results are achieved.

CHAPTER 4 FEM SIMULATION

4.1 Finite element analysis

FEM analysis is applied to the design process to decrease the development time and predict the output patterns, which saves time and production expense. With advancements in computer technology, simulation of complex percolative systems like nanodielectric capacitors has become a reality. The effective properties of the nano composites can be calculated using the finite element analysis, available in COMSOL multi physics. Calculation of the effective permittivity due the metal polymer composite is the goal of this work.

Effective properties of the composite can be calculated by modeling the permittivity using the effective medium theory and generalized effective medium theory or other similar mean field theories [33]. The EMT utilizes various properties of the resultant medium such as shape, size, fraction of inclusions, individual dielectric constants etc to calculate the effective permittivity. The dielectric constant of Polystyrene is 2.6 [23]. The dielectric constant of Silver, which is a noble metal, is calculated using Drude-Loretnz model. The fractions of inclusions were taken from a minimum of 0 to maximum of 1. The EMTs are generally valid only for low volume fractions. For higher values of fractions, the effective properties can also be determined using percolation theory [26]. However determining the percolation threshold is crucial in accurately predicting the properties using percolation theory [37].

4.2 COMSOL Model

4.2.1 Creating the model

The conceptual model of the nano composite is drawn as shown in figure 4.1.

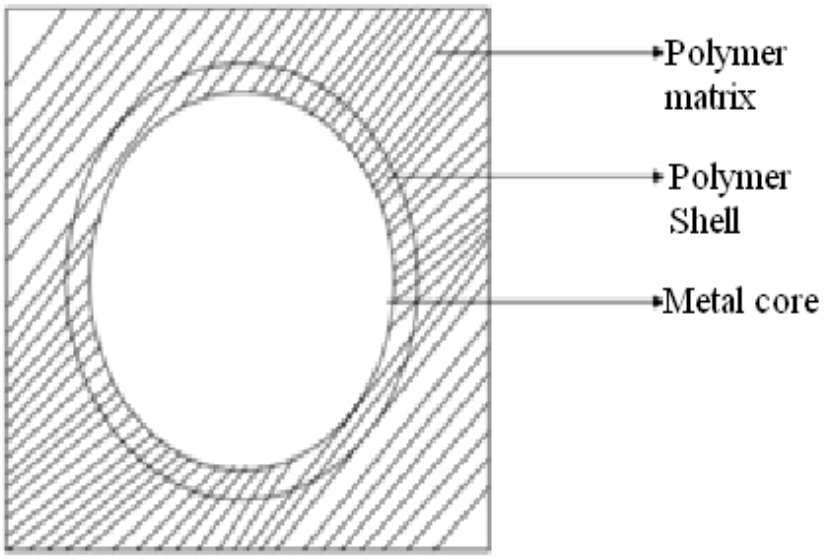

Figure 4.1. Model of the nano metal-polymer composite

COMSOL multi physics allows drawing of a model either in 2D or 3D. The geometry can be drawn using the default tools available in COMSOL or a CAD geometry can also be imported. In our case, since the geometries are as simple as hand drawings, both for the 2D and 3D model, we use the in-built functions of COMSOL. A block of fixed size has to be created and its parameters have to be set according to the polymer characteristics. The properties of silver nano particles are assigned to spheres, which are added inside the polymer block. By varying the number of silver nano particles, we can vary the fraction of loading of the nano particles.

The in-plane electric currents module from the AC/DC modeling is used for this simulation. This model allows simulating the physical entities in the model to be defined as both dielectric and conductor. The electric currents are applied only in the direction of the plane. The magnetic field generated is negligible in this model.

Figure 4.2 shows the geometry setup of a 2D nanodielectric model constituting core nanoparticles with circular disks of core diameter 35 nm enclosed in a rectangular block of fixed area. To analyze the properties of the composite dielectric with varying filler loadings, three geometries are drawn with an increasing fraction of nanofillers. The maximum value of the filler loading is the percolation threshold.

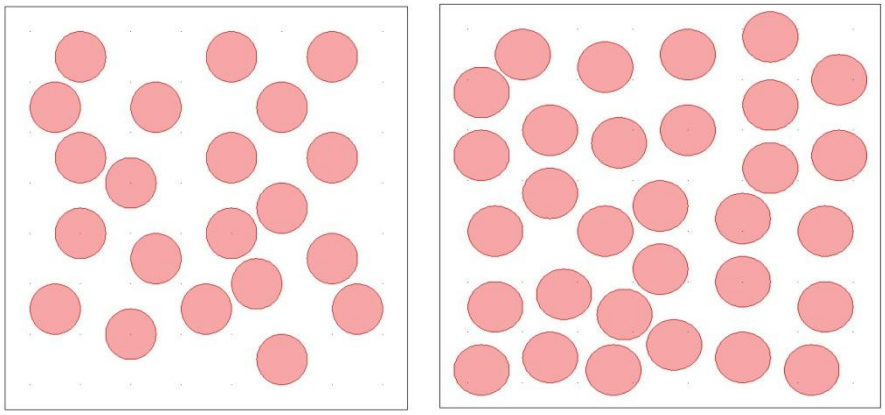

(a) (b)

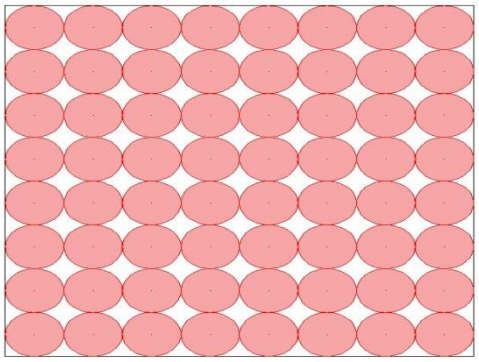

(c)

Figure 4.2. 2D model with (a) f=0.14 (b) f=0.38 (c) f=0.687

Figure 4.2 shows three different fraction of loadings, consisting of 21, 31 and 64 disks. They correspond the fraction of loading of f= 0.14, 0.38 and 0.687. The theoretical value of percolation threshold for 2D model is 0.687, i.e., when circular disks are used [32]. All circular disks are of equal size. They are randomly distributed inside the polymer, since a very uniform dispersion of nano particles in a polymer matrix in unachievable. The size of the polymer block is kept constant for all the three cases.

The 3D model is drawn as shown in figure 4.3. The diameter of the core nano particle is 35 nm. The nano particles are enclosed in a Polystyrene matrix, which is represented by a block.

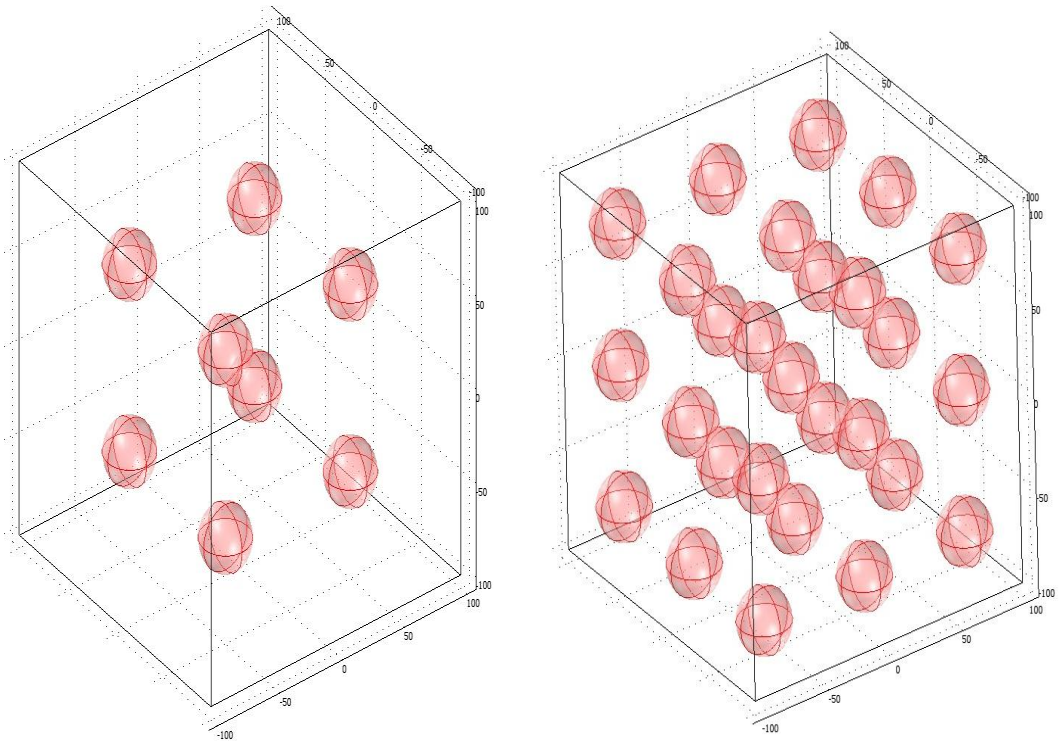

(a) (b)

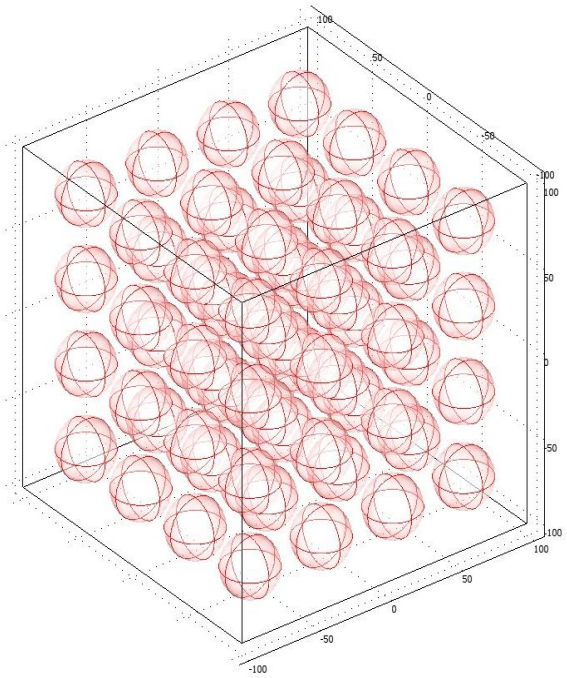

(c)

Figure 4.3. 3D model with (a) f=0.022 (b) f=0.078 (c) f=0.155

Figure 4.3 shows the geometrical setup of a 3D nanodielectric model containing spherical core-shell nanoparticles with a core diameter of 35 nm enclosed in a PVP block of fixed volume. Figures 4.3 (a), (b), and (c) correspond to the three filler volume fractions of 0.022, 0.078, and 0.155 with 8, 27, and 64 core-shell nanoparticles, respectively. The percolation threshold of spheres is 0.16, which is a universally accepted value known as Sher-Zaller invariant [35]. All the spheres in figure 4.3 are at an equal spacing with one another in a block of fixed volume. It is drawn with the help of Array option from Modify option.

4.2.2 Setting up the parameters

The next step after creating the geometry would be to set up the parameters that would define the model. The subdomain settings from Physics menu is chosen to define the electrical properties of the physical models that are to be used.

The subdomain settings describe the physics on a model's main domain, which is divided into subdomains. Different values for each subdomain can be set using settings of the following types:

- Coefficients that define the PDE on the subdomain. The PDE coefficients are available for PDE modes and the weak form modes.
- Material properties, sources, and sinks that define the physics in the subdomain, which are available in the Comsol Module.

The second option is used in this case of modeling, since we have all the data we require. The dielectric constant of the silver nano particles is calculated by using the equation 14. This equation is evaluated during the run time. The equations and constants are declared for the model. Equation $D = \varepsilon_0 \varepsilon_r E$ is chosen, as it is dependent on the electric field and the polarization of the composite. These concepts are considered in the analysis of the simulation results; they are the major governing physics of metal-insulator nanodielectric composite capacitors.

The materials used in the model can also be grouped together in order to define them as the similar entities. In this case, all the spherical or circular nano particles are grouped together and their dielectric constant is calculated during the run time. The electrical conductivity is set up as 63 x 10^{-6}, which is conductivity of Silver. The dielectric constant of the host is defined using the values obtained from the literature

(PS=2.6 and PVP=7). As the core nano particle is coated with the same polymer on which it will be dispersed, there is no need of declaring a separate entity for shell.

After setting up the physical conditions, the next step is to set up the boundary conditions. This set up has to be analogous to a parallel plate capacitor. A capacitor has positive voltage on one end and the other end is grounded. Thus the top face of the model is set for port voltage with a forced input of 1V. The opposite face is set as ground. All other faces are set to periodic continuity, which means that the same region can extend on both the sides.

Thus the final set up of the model resembles as shown in figure 4.4

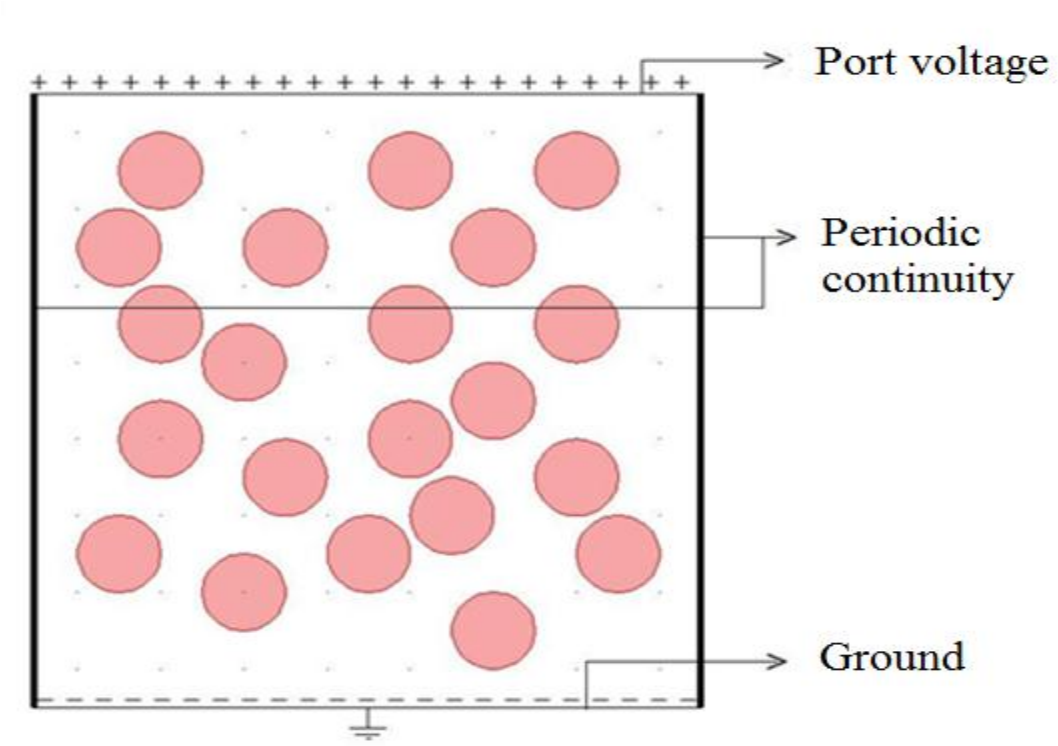

Fig 4.4 Final model of the capacitor

The side faces may also be set as electrical insulation, so that the entire set up acts as a miniature capacitor.

CHAPTER 5. EXPERIMENTAL PROCEDURE

5.1 Preparation of nano particles

The nano particles are synthesized in two stages. The first stage is to synthesize the colloidal Silver nano particle solution and the second stage is to coat it with the stabilizing agent. The stabilizing agent can be a polymer of silica. In order to ensure purity, all the glass-ware that are to be used are cleaned in aqua regia (3:1, HCl/HNO3) for at least one hour, thoroughly rinsed with deionized water and acetone, and then dried in an oven at ~100 ^{o}C prior to use.

5.1.1 Preparation of Silver nano particles

The size-controlled silver nanoparticles are synthesized by a modified polyol method [40]. In this method, PolyvinylPyrrolidone (3g) was dissolved in 75 ml Ethylene Glycol at room temperature, and 100mg (0.6mmol) of $AgNO_3$ was added. The suspension was then stirred at room temperature until complete dissolution of the $AgNO_3$ solution. This solution was heated to 120 **°C** at a constant rate of 1 **°C** /min and then the reaction allowed proceeding for 22 hours. Each sample was cooled rapidly in a water bath until the system reached room temperature, and then 300 ml acetone was added for separating Ag nano particles from Ethylene glycol. The solution was stirred continuously for 30 minutes. The solution was then centrifuged at 7,000 rpm for 20 min, twice and then re-dispersed with ethanol (20 ml). The synthesized nano particles were in the sizes of range 30 nm to 40 nm.

5.1.2 Preparation of $Ag@SiO_2$ core shell nano particles

To coat Ag nanoparticles with uniform silica shells, a modified sol-gel procedure developed by Stöber et al [41] was employed. In this modified procedure, 10 ml from the prepared PVP capped Ag nanoparticles solution described in section 5.1.2 was re-dispersed into a mixture solution of ammonia in ethanol (22ml: 20 ml,ethanol/2 ml, ammonia). The solution is then added with tetraethylorthosilicate (TEOS, 100 µL). The solution was continued to stir for overnight at room temperature. After this procedure, the solution is centrifuged at 7,000 rpm for 20 min, twice and then re-dispersed into ethanol (20 ml). The thickness of the silica shell can be controlled from 20 nm to 70 nm by changing the amount of TEOS. The final size of the nano particles coated with SiO2 was found to vary in the range 150 nm to 180 nm.

5.1.3 Preparation of Polystyrene functionalized nano particles

The silver ion solution (0.03 M AgNO3) was taken in an aqueous state. 30 ml of the solution was mixed with 20 mL of a chloroformic solution of phase transfer catalyst (0.20 M of tetra-octylammonium bromide) and stirred vigorously for 1 hour. The French gray organic phase was subsequently collected, and the chloroform solution (3ml) of thiol-terminated polystyrene (100 mg) was added. The nonanethiol/Ag+solution was stirred for 15 minutes. 24 mL of fresh aqueous Sodium Borohydride (0.43 M NaBH4) solution, used as the reducing agent, was injected. The reaction mixture was stirred for over 3 hours before the organic/nano crystal rich phase was collected. The dispersion phase was washed three times with ethanol to remove the phase transfer catalyst, excess 1-nonanethiol, and reaction byproducts. The mixture was kept for 4 hours at – 22 ^{o}C and

the dark brown precipitate, which was a waste byproduct, was filtered off and washed with ethanol. The crude product was dissolved in 10 ml chloroform and again precipitated with 400 ml ethanol. The final product is the silver NPs in 50 ml chloroform organic solution.

5.1.4 Preparation of NH2-functionalized Ag@SiO2 nano particles

All glassware are cleaned in aqua regia (3:1, HCl/HNO3) for at least 1h, thoroughly rinsed with deionized water and acetone, and then dried in an oven at ~100 ^{o}C prior to use. We synthesized the size-controlled silver nanoparticles by a modified polyol method. In our method, PVP (3 g) was dissolved in 75 ml ethylene glycol at room temperature, and 100 mg (0.6 mmol) of AgNO3 was added. The suspension was then stirred at R.T until complete dissolution of the AgNO3 solution. This solution was heated to 120 °C at a constant rate of 1 °C /min and then the reaction allowed proceeding for 22 h. Each sample was cooled rapidly in a water bath until the system reached room temperature, and then added 300 ml acetone for separating Ag NPs from ethylene glycol (removing EG) and then stirred this solution for 30 min. Centrifuged this solution at 7,000 rpm for 20 min, twice and then re-dispersed with ethanol (20 ml). The surface of metal nanoparticles can be readily coated with uniform silica shells using a modified sol-gel procedure developed by Stöber et al. In this modified procedure, 10 ml from the prepared PVP capped Ag nanoparticles solution described above was re-dispersed into a mixture solution of ammonia hydroxide in ethanol (22ml: 20 ml, ethanol/2 ml, ammonia) and then added tetraethylorthosilicate(TEOS, 50 µL) . The induction period was approximately 45 minutes that the solution color became

cloudy as silica nanoparticles were grown and eventually turned opaque white. 1 ml of (N-acetyl glycyl)-3-aminopropyl-trimethoxysilane, 5% in methanol was then added to the vigorously stirred solution and allowed to react for overnight at room temperature. To promote the covalent bond, this solution was then refluxed for 1h, 90 ^{o}C. These particles are purified by 3 centrifuge cycles at 7,000 rpm for 20 min and then re-dispersed into ethanol (20 ml). The thickness of the silica shell can be controlled from 20 nm to 70 nm by changing the amount of TEOS.

5.2 Preparation of nano composites

A nano composite solution is a solution in which one of the solutes are nano particles. The other solute can be anything that dissolves the solvent. In our case, it is Polyvinyl pyrrolidone. An essential step that determines the characteristic of the dielectric is the nano composite solution preparation, with the correct amount of polymer and nano particles. The polymer is taken in a crucible and weighed. The quantity is adjusted till the required weight of the polymer is obtained. The nano particle solution was sonicated using a micro tip sonicator. The required quantity of the sonicated nano particle solution is taken in a small beaker, using a pipette. The polymer is added to the beaker. The nano composite solution is now heated up to 85 ^{o}C and stirred concurrently, for 25 minutes, in order to achieve uniform mixture throughout the solution. The nano composite solution is now ready for spin coating and other processing.

5.3 Thin film fabrication

Thin film realization is performed a spin coater. The silicon wafer is cleaned before the spin coating step is performed. The spin coating step is followed by metal contact deposition.

5.3.1 Silicon wafer cleaning procedure

Impurities on silicon wafer surfaces occur in essentially three forms:

- Contaminant films
- Discrete particles
- Adsorbed gases that are of little practical consequence in processing

These unwanted contaminants have to be removed before the Si wafer is processed or else we will have more contaminants than materials. The Si wafer is cleaned in two steps. The first step is to sonicate the wafer with chemical cleaners and then dry blow the wafer surface with nitrogen. The Si wafer is taken in a beaker with Trichloro-ethylene, which is a powerful cleaning agent. It is ensured that the Si wafer is completely immersed in the liquid. The beaker is now kept in an ultra sonicator bath for five minutes. The sonicator applies sound energy to agitate the particles on the surface, thus loosening the particles adhering to surface. The solution is now drained and the beaker is filled with Acetone and the same procedure is being followed. It is followed by cleaning with Methanol and Deionized water. The wafer now is blown with compressed dry nitrogen to eliminate the moisture sticking to the surface. The wafer is now clean and hence can be used for further processing.

5.3.2 Spin coating and curing

Spin coating is a process used to form uniform thin films on the top of flat substrates. The machine which performs spin coating is called a spin coater or a spinner. The block-scheme of a spinner is as shown in figure 5.1.

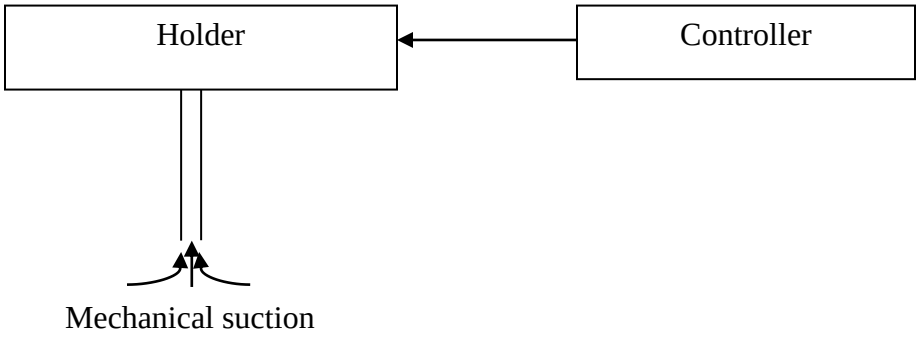

Fig. 5.1. Schematic of a spinner

A suction is used to secure the wafer to prevent it from moving, when acceleration is applied. The controller controls the spinning speed, time and acceleration of the spinner. Any kind of spin coating involves two steps. The first step is the acceleration at slower rate and the second step is the spinning at constant speed to achieve uniform thin layer formation. The wafer is placed more or less center on the top of the holder and held with mechanical suction. The nano composite solution is now deposited at the center of the wafer. The spinner is programmed so that it spins at 100 rpm for 10 seconds, 500 rpm for 10 seconds, 2000 rpm for 20 seconds and 3000 rpm for 30 seconds. This spinning rate has been used, since it resulted in a uniform thin film of the nano composite solution in previous experiments.

Post processing the spin coated wafer leads to a tight bond formation between the Si wafer and the nano composite solution. This leads to increased dielectric strength, since most of the solvent is evaporated and the only material left remaining are polymer and the nano particles, thus forming a very good dielectric. The post processing or curing is generally carried out by heating the sample. The initial heating temperature is 45 ^{o}C. The temperature is increased by 50 ^{o}C for every 5 minutes, till the temperature reached 220 ^{o}C. At 220 ^{o}C, the sample is heated for ten minutes.

5.4 Metal contact deposition

The metal contact deposition is the final stage of the capacitor slab fabrication process. Aluminum metal is used in this case. The use of a metal tip in contact with the dielectric surface, when using a highly doped Si wafer as a substrate, completes the parallel plate capacitor device. The metal contact deposition is established using e-beam evaporation.

5.4.1 E beam lithography chamber

In e-beam evaporation, a beam of electrons, collimated by a pair of deflection coils, are allowed to strike the metal, which is placed at the bottom of the chamber. The metal gets heated up by the incident electrons and starts evaporating. The metal in vapor phase is allowed to deposit on the sample. The chamber is maintained under high vacuum contitions. The starting pressure of the chamber is generally around 4.7 to 5 x 10^{-6} T. A manually controlled shutter is used to control the exposure of the sample to the metal. A quartz control monitoring device (QCM) is used to measure the rate of metal deposition.

Needed inputs to the QCM controller are generally the maerials characteristics such as Density, Z-ratio, etc. The schematic diagram of the e-beam chamber is as shown in figure 5.2.

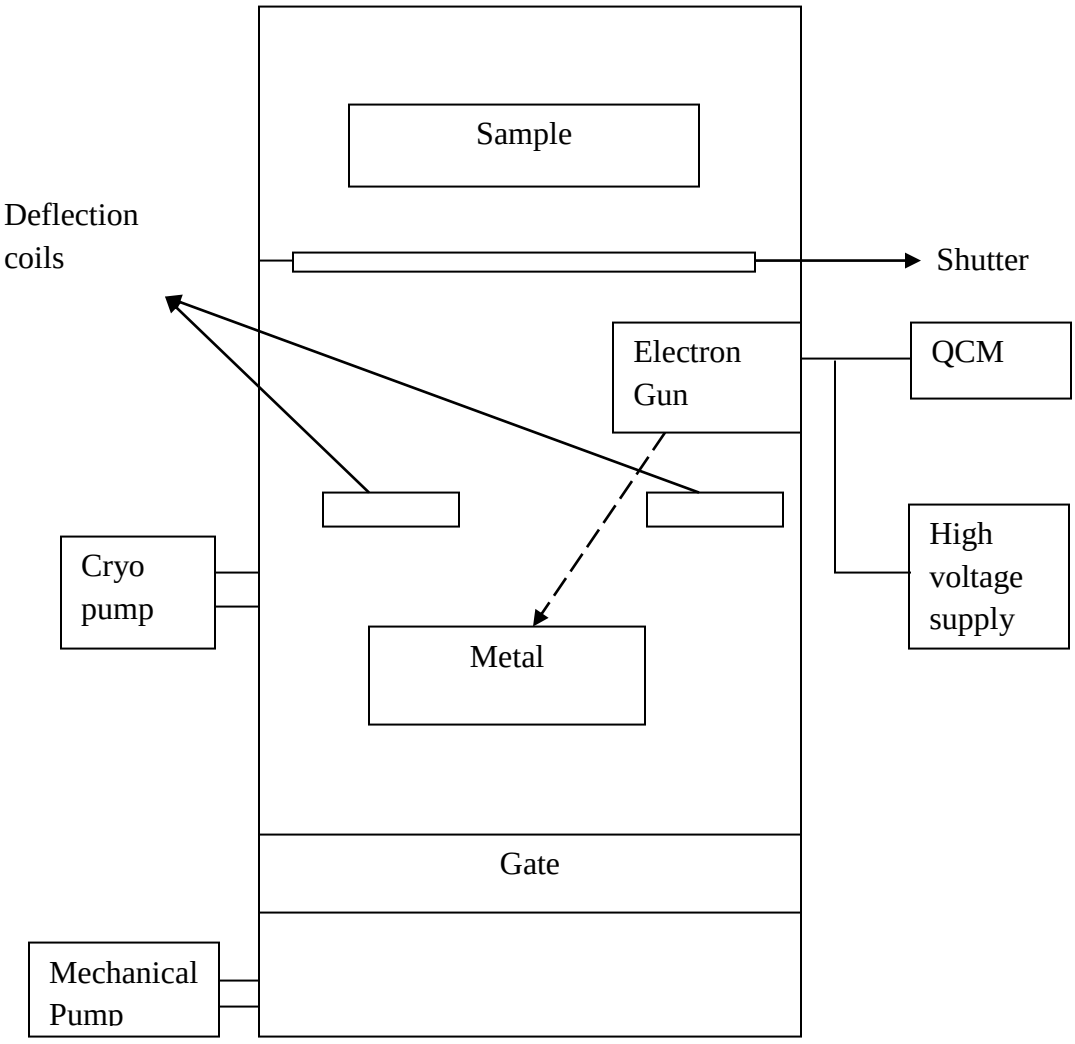

Figure 5.2 Schematic of a chamber for e-beam deposition

5.4.2 Mechanical (Stencil) Mask

A mechanical (stencil) mask is a stainless steel mask with perforations of desired size and shape on it. The mask is used to control the areas of the sample that are to be exposed to metal vapor. In this case, a mechanical mask with 2 mm via is used. Hence after exposure to e-beam evaporation, aluminum metal layer appears on the sample as circular disks of 2 mm diameter. The design schematic of the mechanical mask used in this case is shown in figure 5.3. The mask can be of different size and shape depending on the requirements.

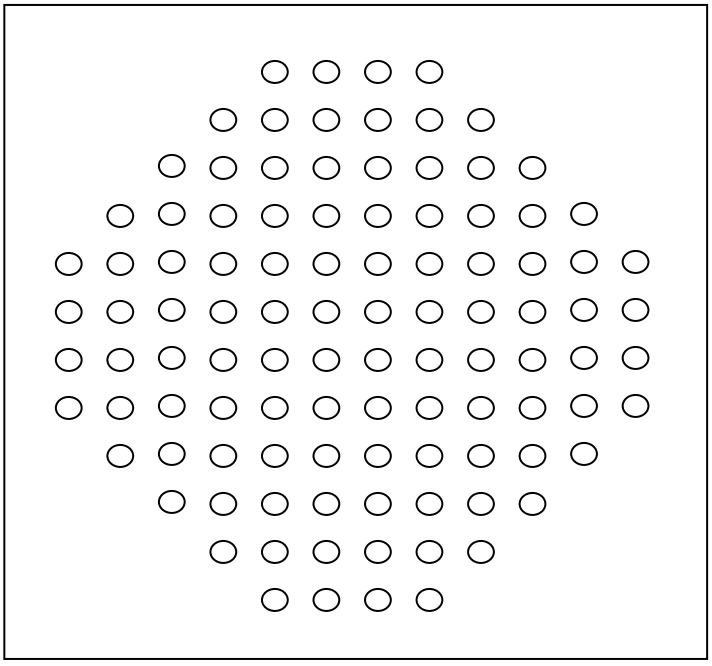

Figure 5.3. Design of the mechanical stencil mask (approximate scale)

The sample is placed beneath this mask and clamped to the holder. This setup is then placed in the e-beam chamber and then evaporation is performed.

5.4.3 E-beam deposition procedure

The gate valve of the chamber is closed first. The chamber is filled with nitrogen and then it is vented. When the air flow is felt on the sides of the chamber, the lid is hoisted up. The sample with the mask is placed on the top of the sample holder, ensuring that it is in line with the aluminum crucible. The lid is hoisted down and the mechanical pump is turned on to reduce the pressure. The pressure should reach $30x10^{-3}$ Torr. If the pressure doesn't come down, it is due to the contaminants like moisture, which had accumulated, when the lid was hoisted up. They can be eliminated by venting the chamber with Nitrogen and then the pressure is reduced again. The mechanical pump is now turned off and the power supply is turned on. The electron emission current on the power supply is set all the way to zero. The shutter is closed so that no part of the sample is exposed to metal. The high voltage and the deposition controller of the QCM are now turned on.

The deposition rate is set as 1Å/s. The reading in the deposition controller is set to zero. Now the shutter is opened. The deposition rate is maintained at 1Å/s for first 100 Å thicknesses. This ensures a very uniform metal layer on the top of the sample. The uniformity of the next layer of metal deposited on top greatly depends on the uniformity of the first 100 Å thicknesses. The deposition rate is gradually decreased when the desired thickness of metal is achieved. The shutter is closed completely and the deposition controller is switched off. The e-beam power supply is turned off and the chamber is allowed to cool for three hours. The lid can then be hoisted up to take the sample outside.

Figure 5.4 shows the schematic cross-section of the final fabricated capacitor.

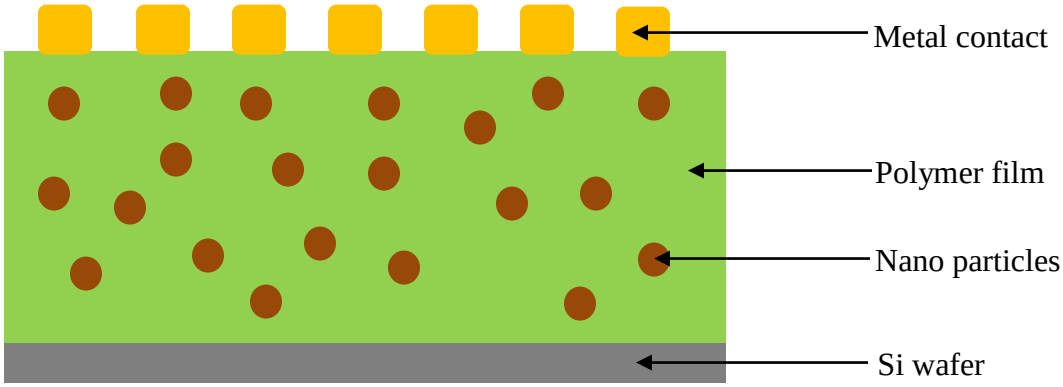

Figure 5.4 Cross-section of a fabricated capacitor

The final fabricated capacitor can now be tested and characterized. The I-V characteristics and the breakdown voltage of the capacitor can be determined.

CHAPTER 6. RESULTS AND FUTURE WORK

The step-by-step fabrication procedure described in chapter five was followed by a study on the device performance and its characteristics. In this chapter, the theoretical, simulation and the practical results are discussed and compared. The dielectric constant, quality factor and the breakdown voltage are considered as electrical characteristics. Nanoparticle arrangement in the microstructure is considered in structural analysis. The thickness of the nano dielectric is determined using Scanning Electron Microscopy (SEM). The size-dependent dielectric constant of Ag is calculated for a range of frequencies using the Drude-Lorentz model. The effective dielectric constant of the composite is calculated using EMTs and the percolation theory, discussed in Chapter 3. Varying concentrations of the nano particles are implemented using the COMSOL multiphysics software, both in 2D and 3D modes. The simulation is performed and the distribution of the electric field, electric displacement and the dielectric polarization is analyzed and discussed.

6.1 Theoretical results

6.1.1 Drude-Lorentz's model calculations

The Drude-Lorentz's model was implemented to determine the size dependent dielectric function of silver. The diameter of the nano particles was considered as 35 nm, which is less than the mean free path of Silver atoms (40 nm) [5]. The size-dependent dielectric constant of 35 nm Ag cores was calculated from Equation 14. The modified scattering time and damping factor of a 35 nm silver particle were calculated using Equation 13, and their values were obtained as $3.77*10^{-14}$ seconds and $1.088*10^{14}$ Hz,

respectively. Figure 6.1 and 6.2 show the plots between the real and imaginary parts of the dielectric constant of Silver with varying frequency. These values for the dielectric functions of Silver are used in EMT calculations.

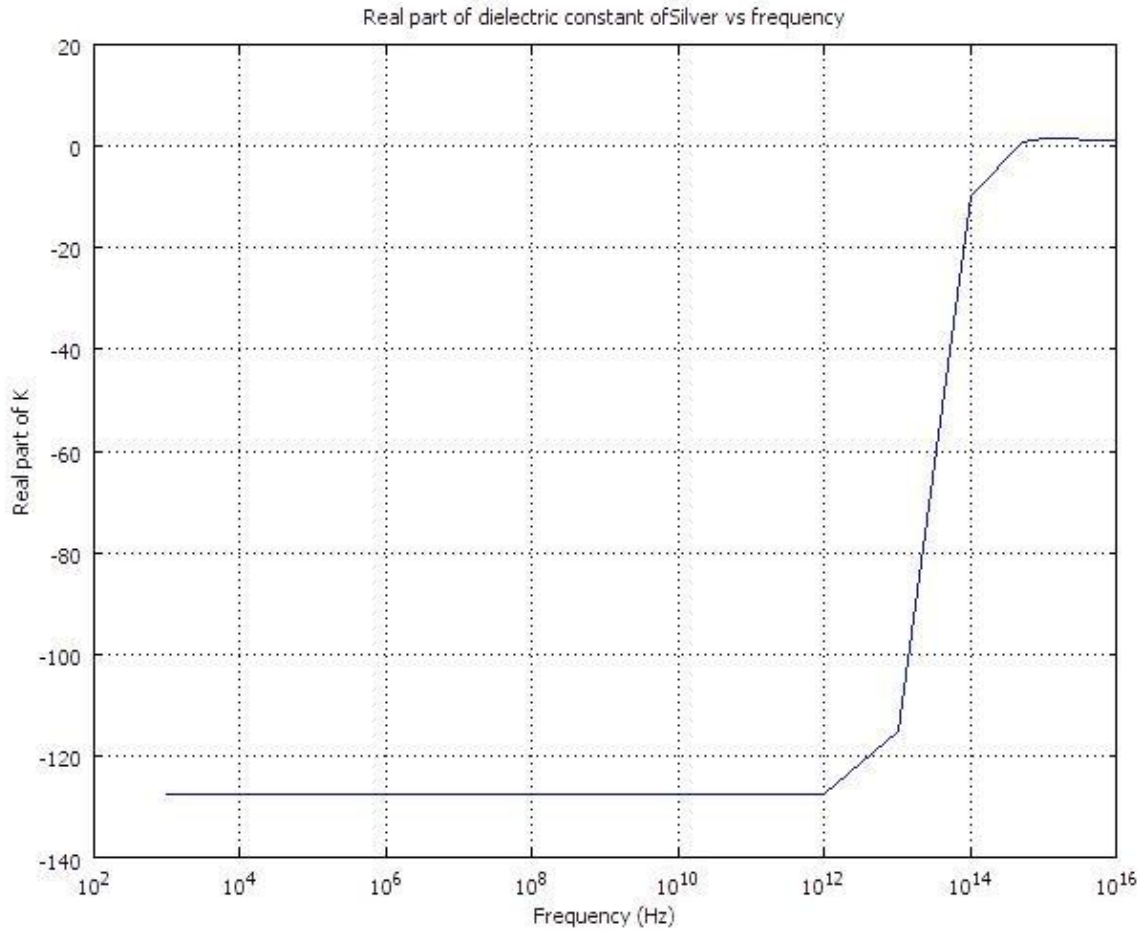

Figure 6.1 Real part of dielectric constant of Silver vs. Frequency

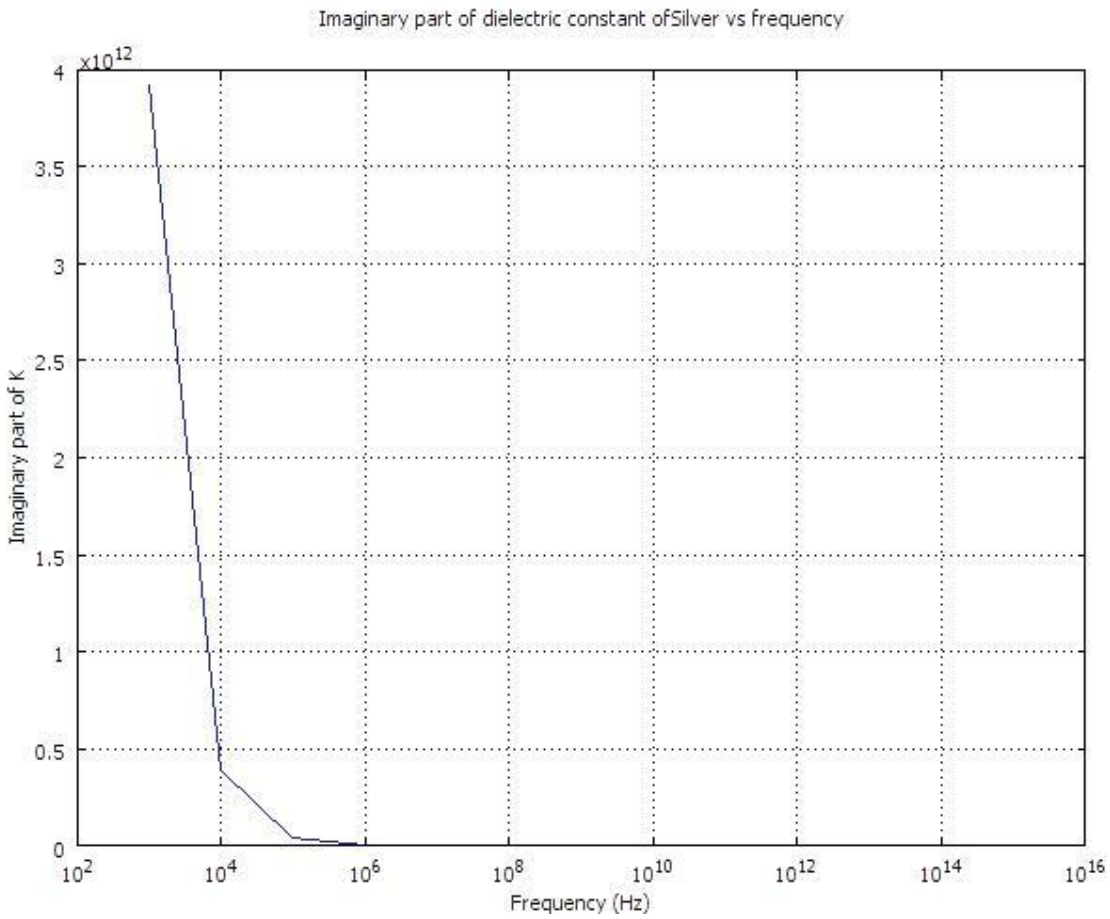

Figure 6.2 Imaginary part of dielectric constant of Silver vs. Frequency

It can be seen that the real part of the dielectric constant of Silver is negative at very low frequencies. At such frequencies, the electrons don't have enough time to align themselves in the direction of the electric field. Instead, they start conducting immediately. Thus at higher frequencies, the electrons have enough time to align themselves and some times, the relaxation time may also be included. Thus the tend to exhibit positive dielectric constant at higher frequencies.

6.1.2 Effective Dielectric constant using EMT

The effective medium theories are used to calculate the effective dielectric constant of the nano composite, i.e., including the dielectric constant of the polymer and the size dependent dielectric constant of Ag nano particles, calculated using the Drude-Lorentz model.

The plot in figure 6.3 gives a comparison between the dielectric constant calculated using different effective medium theories. All the models give the same K value at low fraction of loadings. In case of Loyenga model, the contrast between the host matrix and the inclusions shouldn't be very high. But in case of the polymer and the Ag nano particles, they have very high contrasting properties, which make the Loyenga model unsuitable for this application. EMTs are generalized theories and cannot be considered for exclusive properties of the metal/polymer composites. For the same reason, the effective dielectric constant of the metal/polymer composites cannot be predicted accurately by the EMT models. EMTs are valid only in the low-volume limit [4].

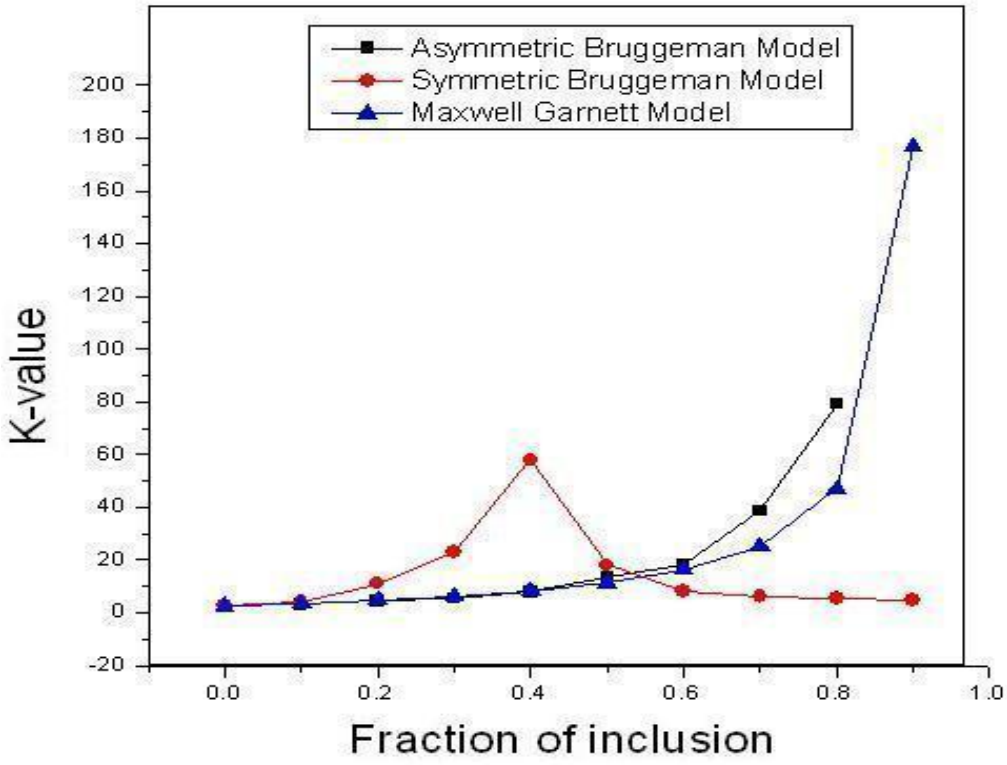

Figure 6.3 Real part of dielectric function of a 2D model with Ag fillers in PVP matrix

6.1.3 Percolation theory predictions

The fraction of loading is major factor that increases the dielectric constant of the polymer-based capacitor, using percolative composite techniques. As mentioned earlier, the effective dielectric constant of the composites can be increased dramatically when the fraction of loading of the nanofillers is close to the percolation threshold. In the previous work, a two-hundred times increase in the dielectric constant of the PVP matrix was seen when the loading of the nanoparticle neared the percolation threshold through COMSOL multiphysics simulations [4]. When the same percolation theory was used to implement Ag nano particles in Polystyrene matrix, the dielectric constant was increased 1000 times than that of its original value.

Percolation theory, unlike EMTs, considers the metal/insulator nature of the Ag/PVP composites. According to percolation theory, a super capacitor network is formed at the percolation threshold because of the difference in conductivities of the metal and insulator in the composite. This difference is taken into account by percolation theory, which predicts an increase in the effective dielectric constant at the percolation threshold [4]. The effective dielectric constant calculation in this work, therefore, is predicted accurately by the percolation theory. The COMSOL multiphysics simulations show an increase in the net electric field and polarization of both the 2D and the 3D composites when the loading of nanoparticles is near the percolation threshold. At percolation threshold, the effective dielectric constant for 2D and 3D composites is calculated as 1400, which is a 200 times increase as compared to the dielectric constant of PVP. Similarly, for the PS polymer, the K value reaches 2600, whereas for pure PS, it is just 2.6.

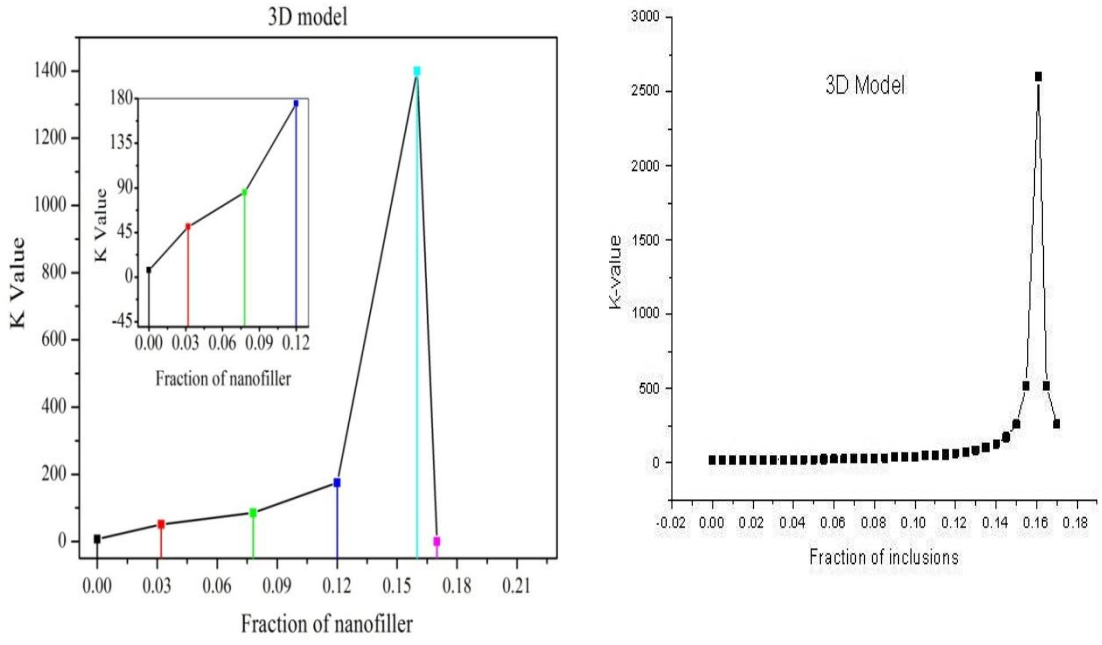

(a) (b)

Figure 6. 4 Comparison between K-values predicted using Percolation theory of PVP matrix and PS matrix

The plot in figure 6.4 shows the K value predicted using the percolation theory equations. The K value can be calculated in both the 2D and 3D models. Since 3D model is more practical in implementation, only the plots is 3D have been shown. It can be interfered that as the fraction of loading reaches the threshold value, the K value reaches it maximum. At zero percent loading, the nano composite solution is pure polymer, thus the effective K value is same as that of the pure polymer. As the fraction of loading increases beyond the percolation threshold, the polymer has more metal nano particles, thus the solution becomes more like a metal. So the effective K value decreases.

6.2 Simulation results

The simulation was done in both the 2D and 3D modes using the models explained in chapter 4. The electric field, polarization and the electric displacement inside the capacitor is studied. The electric field and polarization, formed the same distribution, but for the values. Hence only polarization is discussed. The electric displacement and polarization, inside the dielectric varied as the fraction of loading varied.

6.2.1 2D Model results

The plot of Ag/PS has been explained below.

(a) Electric polarization

The plot of electric polarization inside the capacitor has been drawn as shown in figure 6.5.

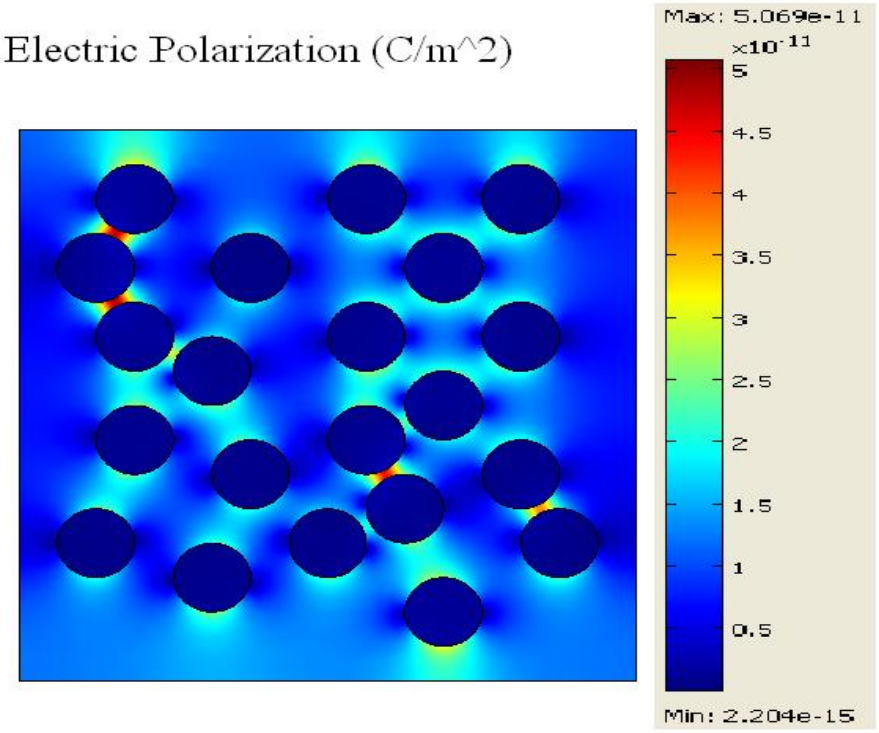

Figure 6.5 (a) Electric Polarization in 2D with f=0.14

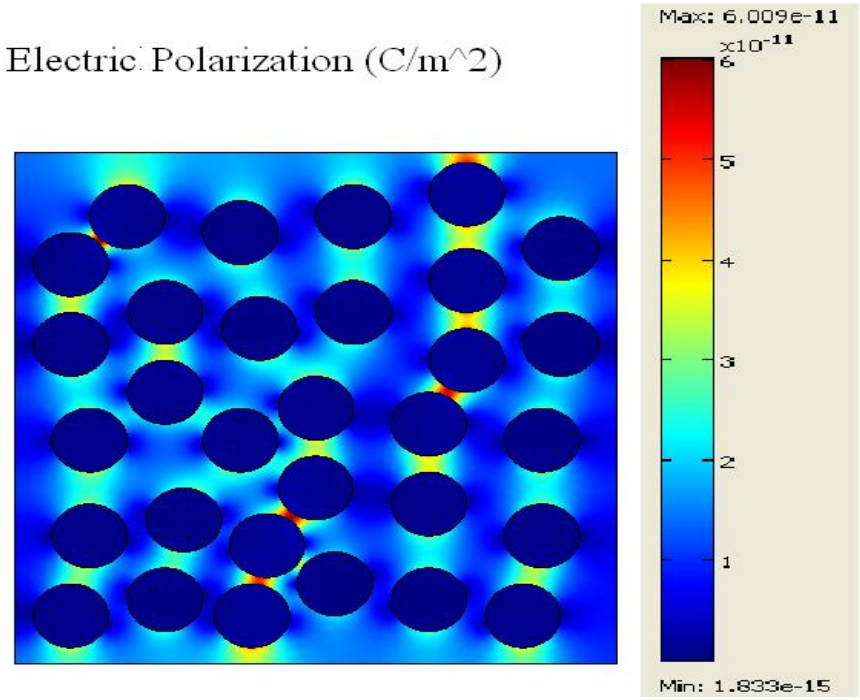

(b)

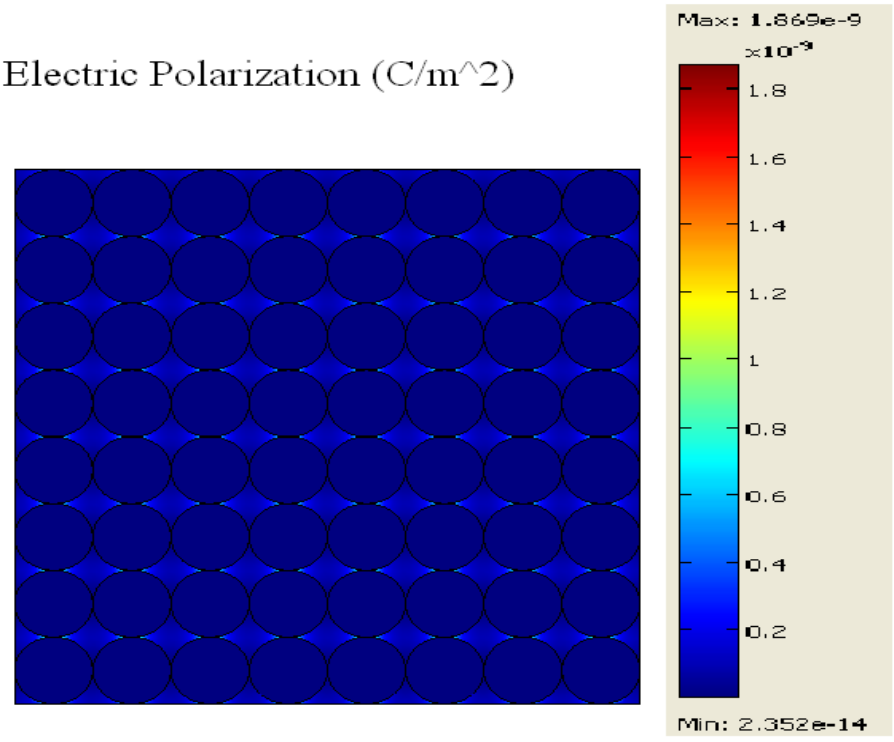

(c)

Figure 6.5 (b) and (c); Electric polarization with f=0.38 and 0.687 respectively

(b) Electric displacement

The plot of electric polarization inside the capacitor, obtained by the simulation is as shown in figure 6.6

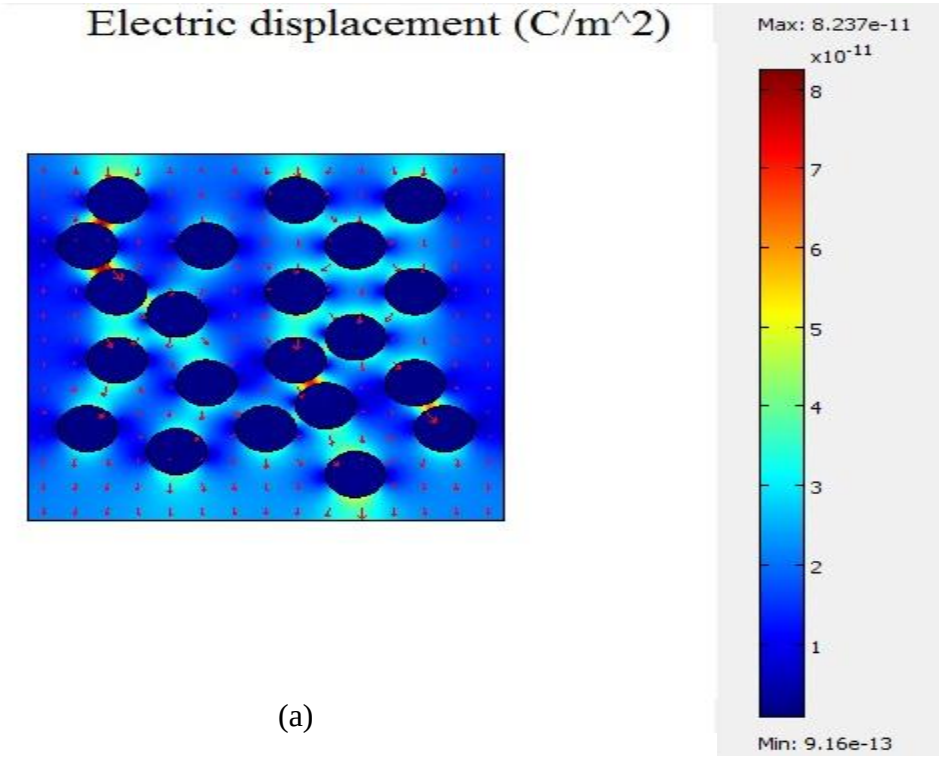

(a)

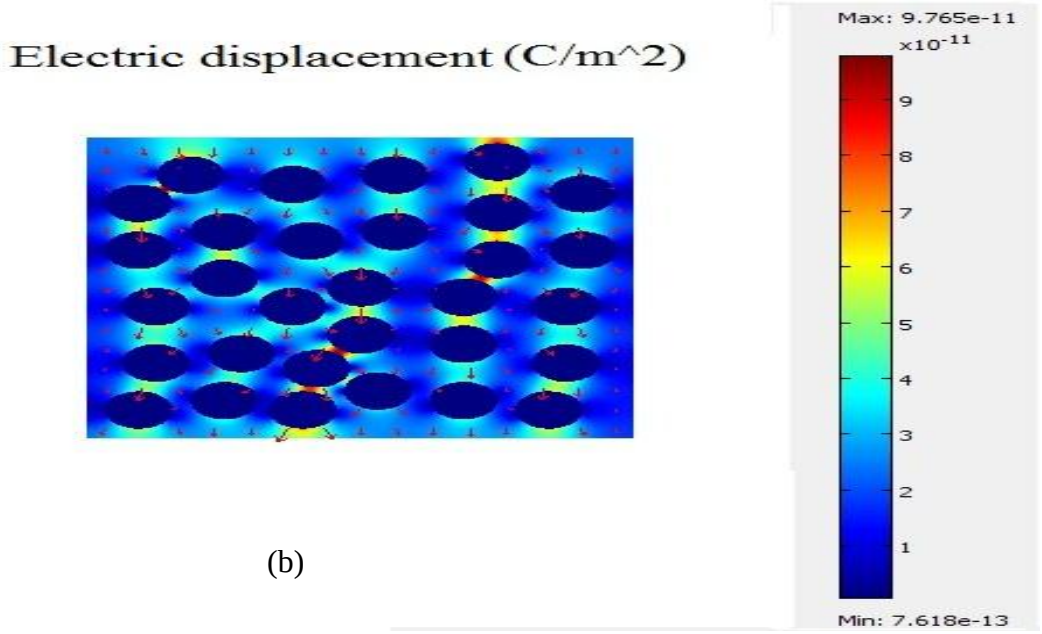

(b)

Figure 6.6 (a), (b) Electric displacement with f= 0.14 and f=0.38 respectively

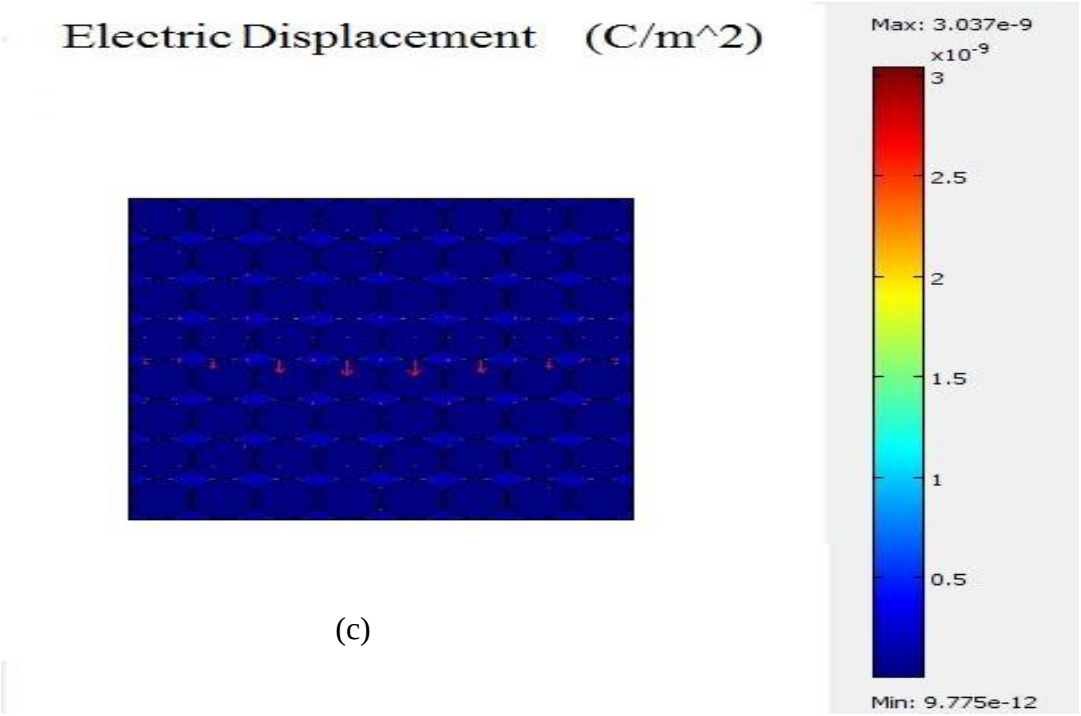

(c)

Figure 6.6 (c) Electric Displacement with f=0.687

When the nano particles are embedded in the Polystyrene matrix, an electric field is generated inside the matrix, which acts in the direction opposite to that of the surface charge and applied field. This is due to the reason that the positive charges in the nano particles are attracted towards the negative charges on the polymer surface. This is also the reason for high electric polarization, near the polymer-metal interface. The illustration of this concept has been shown in figure 6.7.

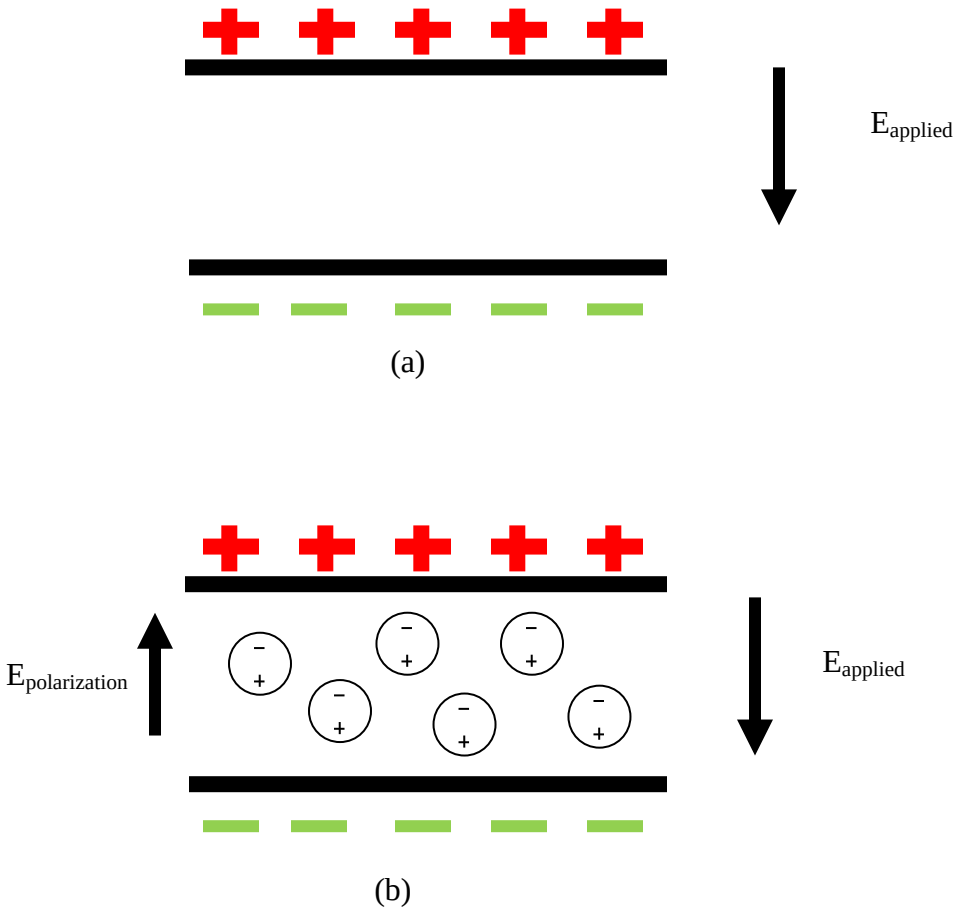

Figure 6.7 Increase in Polarization due to metal fillers

The effective Electric field is given by

$$E_{effective}=E_{applied}-E_{polarization}. \quad (22)$$

The capacitor equation for an applied voltage is given by

$$C = \frac{q}{V}. \quad (23)$$

The Electric field equation is given by

$$E = \frac{V}{d}. \quad (24)$$

The capacitance is thus given by

$$C = \frac{q}{E.d}. \tag{24}$$

The effective electric field inside the capacitor decreases, due to the inclusion of metal nano fillers. Thus the capacitance of the capacitor increases.

The total polarization equation is given by

$$P_{total}=K_{eff} \text{ x } E_{eff}. \tag{24}$$

As the effective field increases and the polarization decreases, the only increasing factor according to the equation, should be K_{eff}.

The electric displacement of the dielectrics which has Ag nano particles in PVP matrix also follows the same pattern, which is shown in figure 6.8.

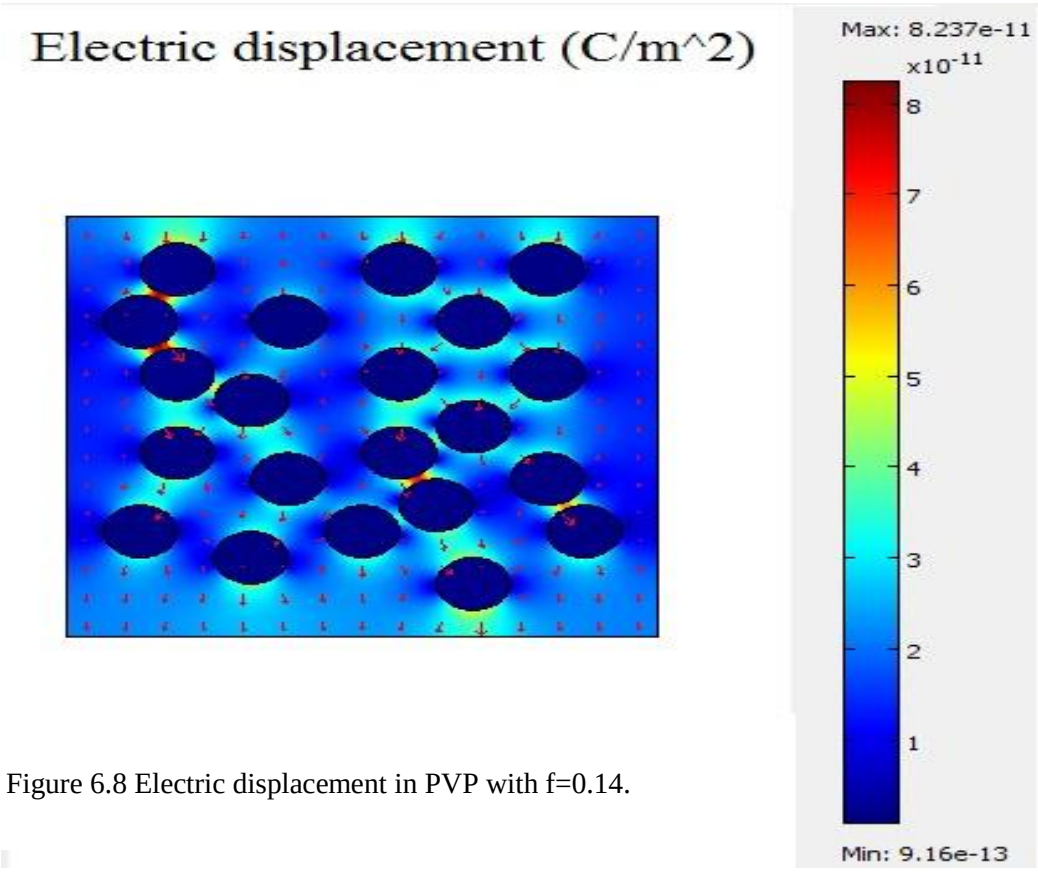

Figure 6.8 Electric displacement in PVP with f=0.14.

6.2.2 3D Model results

In order to determine the nanocomposite characteristics in 3D, three geometries were drawn with loading fractions of 0.022, 0.078 and 0.155 which corresponds to 8, 27 and 64 spheres. The same boundary and subdomain conditions mentioned in Section 3, apply to 3D model too. A value of 0.16, known as Sher-Zaller invariant [35] has been universally accepted as percolation threshold for a homogeneous composite with spherical fillers of the same size. The same value has been used as the percolation threshold for this modeling.

The slice plots showing the polarization and electric field in the 3D domain has been drawn as shown in figure 6.9 and 6.10, respectively.

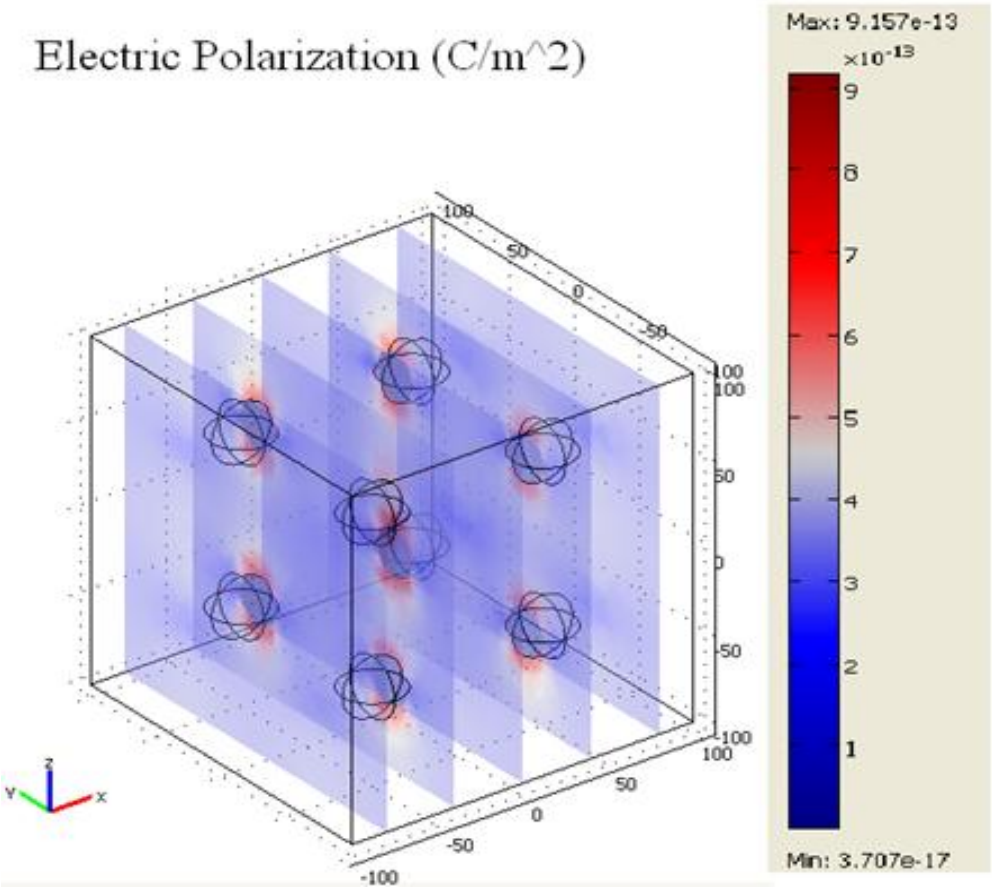

Figure 6.9 (a) Electric polarization with f=0.022

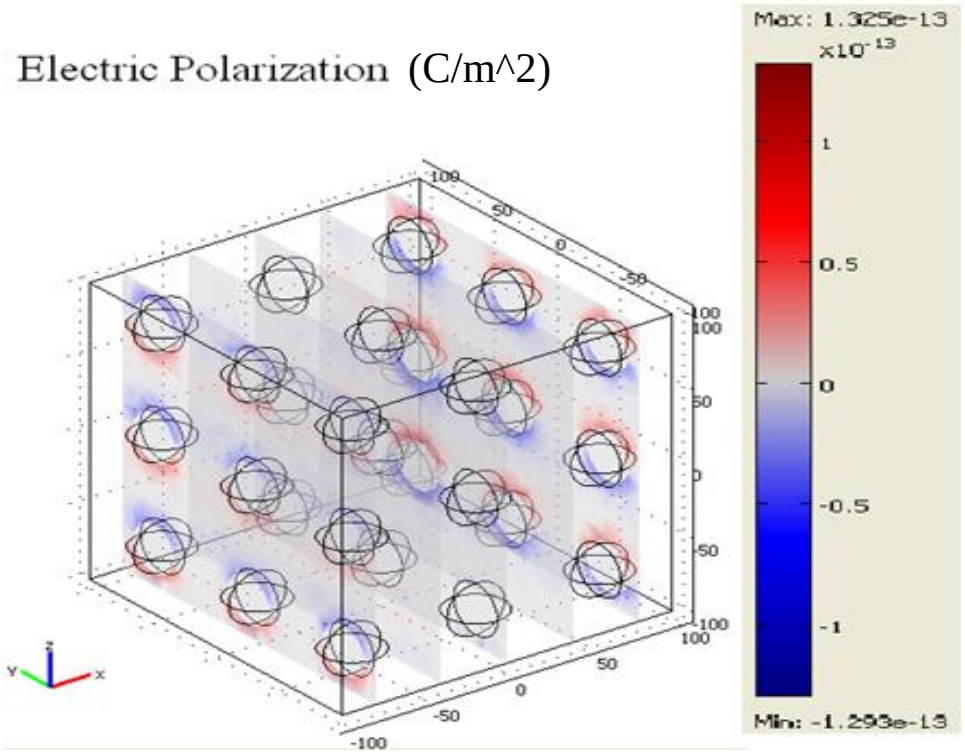

(b)

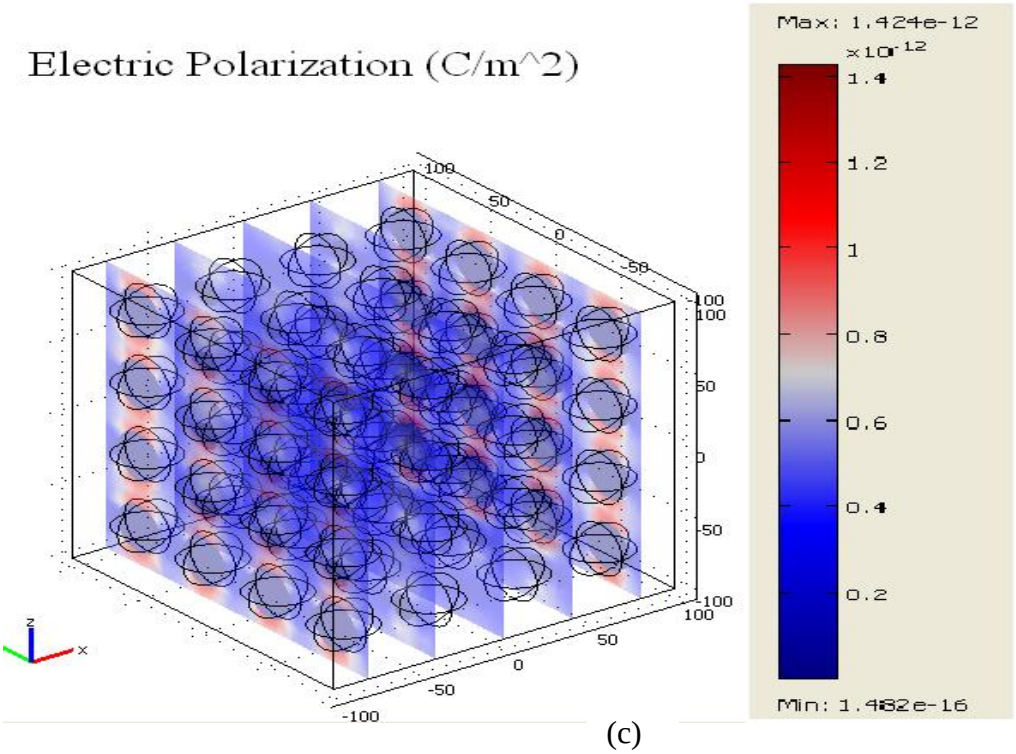

(c)

Figure 6.9 (b) and (c) Electric polarization with f= 0.078, 0.155, respectively

The electric polarization in 3D model follows the same pattern as of the 2D model. The effect of polarization is maximum near the metal-polymer interface. It can be seen that the polarization value increases as the fraction of loading increase. The maximum polarization value was 9.157×10^{-13} for f=0.022 and for f= 0.155, the value was 1.424×10^{-12}. The plot of the electric displacement in 3D model is as shown in figure 6.10

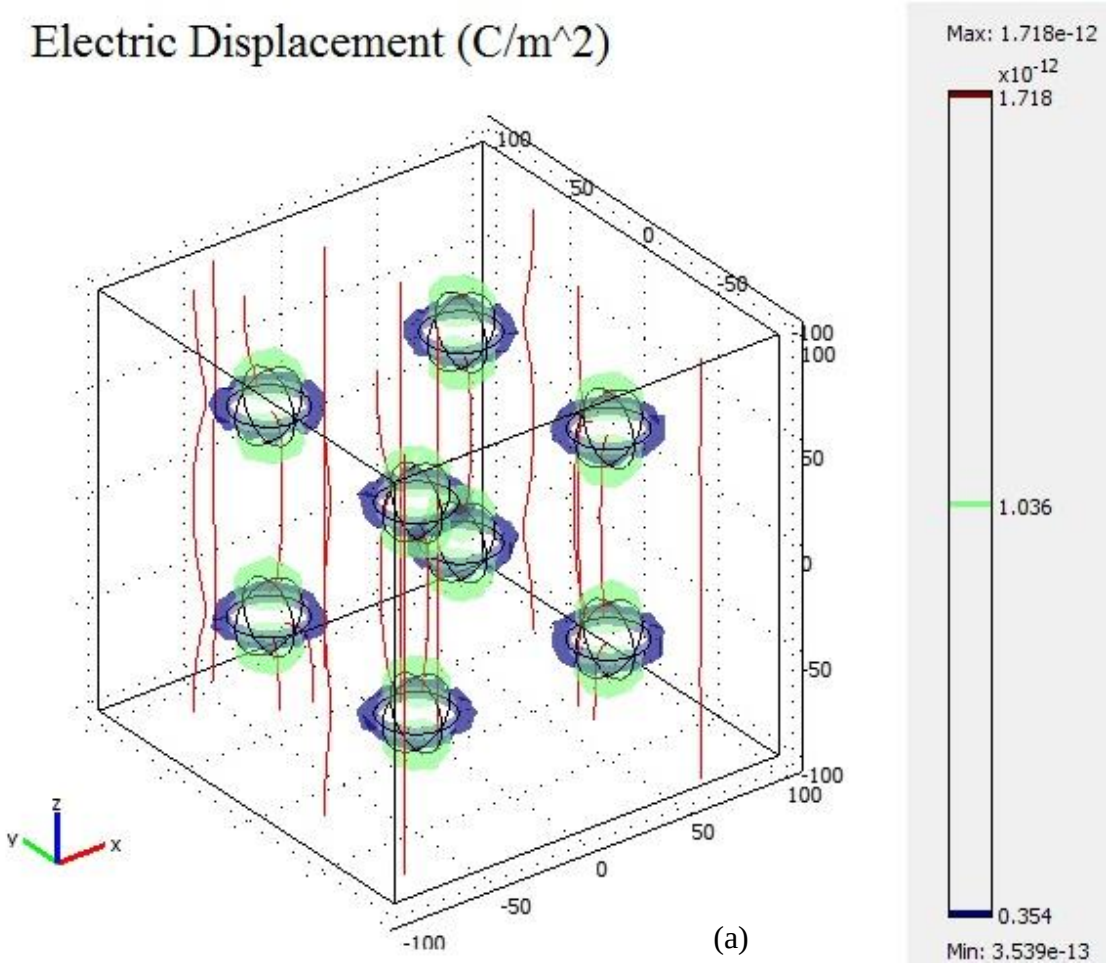

Figure 6.10 (a) Electric displacement with f=0.022

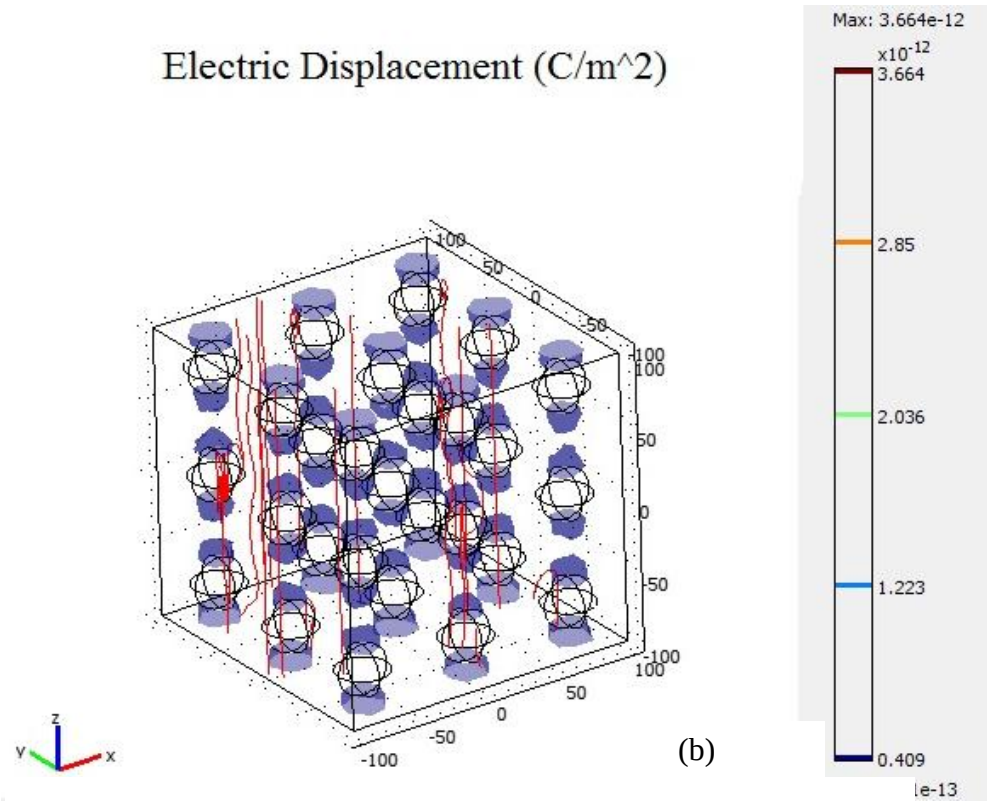

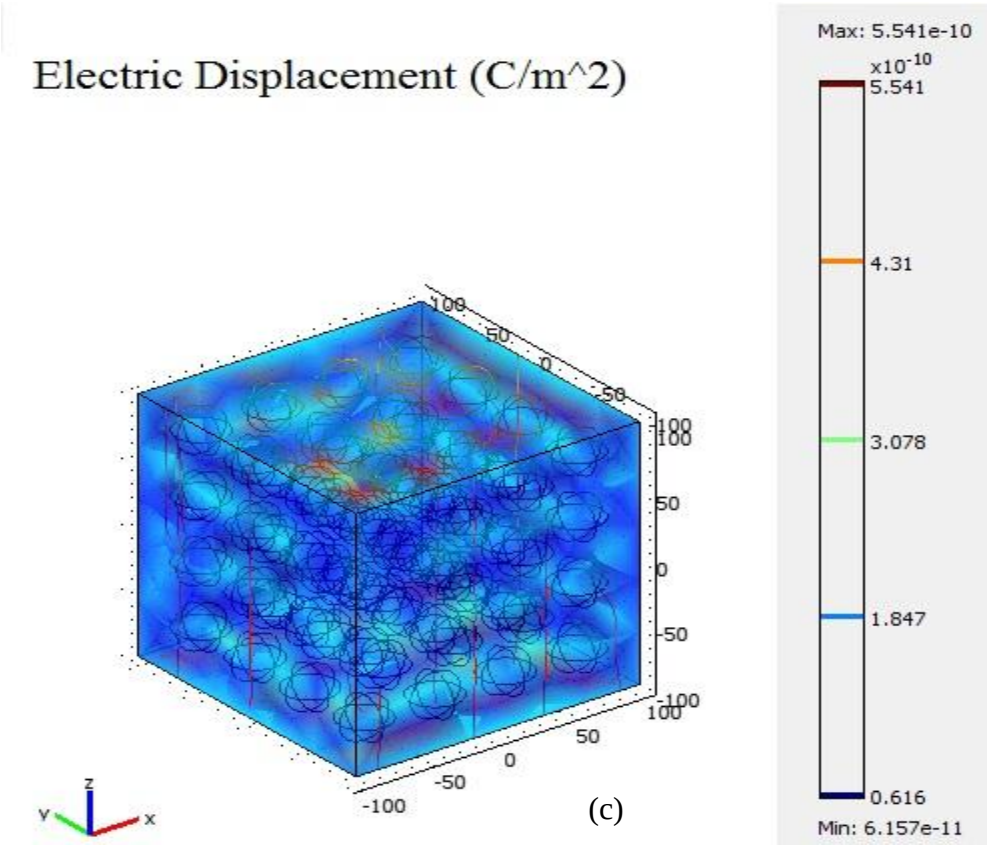

Figure 6.10 (b) and (c) Electric Displacement with f=0.078 and f=0.155, respectively

6.3 Experimental Results

The thin films were developed on a quarter of a two-inch wafer using a Laurell Technologies WS-400 spinner. The Al contacts of 2mm-diameter circular spots were deposited using a mechanical mask in an e beam evaporator. The thickness of the dielectric film was measured using an FEI XL30FEG SEM. The capacitance measurements were conducted using a HP 4275A LCR meter (10 KHz-10 MHz) and also with an HP 4284A LCR meter (20 Hz-1 MHz). The dissipation factor was also recorded from an LCR meter. The quality factor is the inverse of the dissipation factor. It serves as an index to compare the quality of different materials with similar dielectric constants.

I-V measurements were obtained from a Keithley 6487 picoammeter/voltage source controlled using the Labview software to supply the input voltage and to read the output current. I-V measurements of leakage current were measured when a voltage was applied across the capacitor terminals. The voltage applied was increased until the current reached a value of 2.5 μA; this voltage was called the breakdown voltage. Input voltage was increased beyond the breakdown voltage to find a value of the voltage that the device can withstand before it forms a short circuit. The maximum voltage that can be applied using the Keithly 6487 was 500 V.

6.3.1 Characteristics of pure PVP

In order to determine the break down voltage and the K value of pure PVP, which will be used in the experiment, thin films were formed on the Si wafer using PVP dissolved in ethanol solvent. The amount of the polymer used, quantity of solvent and its electrical characteristics have been shown in table 6.1

Table 6.1 Properties and characteristics of capacitors made out of pure PVP

Quantity of PVP (g)	0.2	0.4
Quantity of ethanol (ml)	2	3
Spinning speed	10 seconds 100 rpm 10 seconds 500rpm 20 seconds 2000 rpm 30 seconds 3000rpm	10 seconds 100 rpm 10 seconds 500rpm 20 seconds 2000 rpm 30 seconds 3000rpm
Curing temperature	225^{o}C	225^{o}C
Thickness (nm)	590	600
Capacitance (pF) at 10 KHz	19	31
Dielectric constant	4.03	6.7
Dissipation factor	0.01	0.01
Breakdown voltage (V/µm)	>84.74	62.5

The spinning speed and curing temperature were stabilized from the previous work one with the same pure PVP polymer in ethanol solvent [4]. The obtained K value 6.7 is close to 7, which has been determined as the K value of PVP according to research [42]. Both the samples were able to withstand an applied voltage of 500 V, without any short circuit. At 225 ^{o}C, the cross linking of the polymer with the wafer is very good and hence the same temperature was used as the curing temperature for further samples with nano particles in it.

6.3.2 Characteristics of Ag nano particles in PVP

The Ag nano particles coated with SiO_2 and Polystyrene were used for preparation of the nano dielectrics. The nano particles were suspended in ethanol solvent. The polymer matrix was pure PVP. These nano dielectrics were used in fabrication of capacitors and their electrical characteristics were studied. The statistics of the electrical properties of these capacitors are as shown in table 6.2.

Table 6.2 Properties and characteristics of capacitors made with Ag nano particles in PVP

Quantity of PVP (g)	0.4	0.4	0.4	0.4	0.4	0.4
Quantity of Nano particle solution (ml)	3	2.5	3	4	4	4
Stabilizing Shell	PS	PS	SiO_2	SiO_2	SiO_2	SiO_2
Curing temperature (^oC)	225	225	225	225	45 to 225 (increased in steps of 50^oC for every 5 mintues)	45 to 225 (increased in steps of 50^oC for every 5 mintues)

Table 6.2 (contd.) Properties and characteristics of capacitors made with Ag nano particles in PVP

Capacitance at 10 KHz (pF)	72	20.2	74	43	130	157.3
Dielectric constant	9.06	2.54	9.31	5.41	28.65	32.82
Dissipation factor	0.02	0.055	0.01	0.01	0.01	0.08
Breakdown Voltage (V/ µm)	31	86.2	38	71.38	86.2	>86.2
Shorted Voltage (V)	180	500	250	414	500	Did not short at 500V

The sample was post baked at a high temperature of 225 ^{o}C, immediately after the spin coating. Since the sample still had the solution in liquid phase on the top of the wafer, such a sudden high temperature caused streaks to develop on the thin film. In order to avoid it, the sample was cured at a slower rate, starting from 45 ^{o}C to 225 ^{o}C, increasing in steps of 50 ^{o}C for every 5 minutes. This led to uniform distribution of heat throughout the surface and hence formation of any air bubble or streak was avoided. This led to improved electrical characteristics of the capacitor. All the samples were

considered to have uniform thickness throughout the surface. The thicknesses of all the samples were normalized to a value of 5.8 microns.

6.4 Modified procedure

The nano particles synthesized by the process mentioned in chapter 5 were cumbersome in determining the concentration. Hence the fraction of loading of the nano particles in the polymer matrix was hard to determine. Thus comparison between the theoretical results and the experimental results was not possible. The commercially available nano particles, with known concentration, were utilized for producing nano dielectrics. The nano particles were of concentration 0.02 mg/mL. The nano particles were suspended in water solvent. Thus a new procedure was designed to synthesize the nano dielectrics.

6.4.1 Determination of concentration of polymer required

The amount of polymer in the solvent determines the viscosity of the solution. Higher the quantity of the polymer is, more is the viscosity. An experiment was performed to determine the minimum amount of the polymer required for a proper coating on the Si wafer. Five different quantities of polymer 1 g, 2 g, 5 g, 10 g and 20 g, were added to 10mL of water. The zeta potential and the pH value of the water used to suspend nano particles were -35.6 mV and 7.8 respectively. The pH value of laboratory H_2O was close to 4. Hence required amount of base, Sodium Hydroxide was added to water, to increase the pH level.

The Si wafers, on top of which the polymer solution was to be spin coated, were treated with ozone, to make the wafers, more hydrophilic. Thus five different samples were synthesized, which had different loadings of polymer in water. The sample with highest quantity of polymer, i.e., 20 g, was more viscous and hence it formed a very good layer on the Si wafer. The thin film on the Si wafer with 1 g of polymer was barely visible. The adequate amount of polymer, which formed a clean thin film on Si wafer, was the one with 10 g. Hence it was determined that for a proper thin film layer formation, we need to use at least 1% loading of polymer.

6.4.2 Increase in fraction of loading

The basic idea of increasing the concentration without leading to nano particle agglomeration and also a good viscous solution is to perform a slow evaporation of the solution. 2 mL of the solution which has 0.04 mg of nano particles was taken in a vial. The solution was added to 100 mg polymer and stirred with the help of a magnetic stirrer. The polymer was allowed to completely dissolve in the solution. The evaporation rate of any solution depends on the surface area. The larger the surface area is, the higher the evaporation rate is. Hence a flat beaker was taken and the solution was transferred from the vial to the beaker.

The 2 mL of the solution was weighed along with the box and the total weight is noted. From this the weight of the solution is calculated. The beaker is now kept in a desiccator, under vacuum. The weight of the box was noted at certain time interval. The solution is let to evaporate till the required concentration was achieved. In our case, we could achieve a concentration of 0.04 % loading. The sample was then post baked with a

starting temperature of 45 ^{o}C, till it reached 225 ^{o}C. The temperature was increased at the rate of 50 ^{o}C for every 5 minutes. The following table shows some of the important results that were obtained from the samples with the modified procedure.

Table 6.3 Properties and characteristics of capacitors made with Ag nano particles in PVP with modified procedure

Quantity of PVP (mg)	100	200	200
Quantity of Nano particle solution (ml)	2	4	4
Stabilizing Shell	PVP	PVP	PVP
Ozone treatment	Yes	No	Yes
Spinning Speed	10 seconds 100 rpm 10 seconds 500rpm 20 seconds 2000 rpm 30 seconds 3000rpm	45 seconds 300 rpm 45 seconds 2000 rpm	45 seconds 300 rpm 45 seconds 2000 rpm

Table 6.3 (cont.) Properties and characteristics of capacitors made with Ag nano particles in PVP with modified procedure

Curing temperature (^oC)	45 to 225 (increased in steps of 50^oC for every 5 mintues)	45 to 225 (increased in steps of 50^oC for every 5 mintues)	45 to 225 (increased in steps of 50^oC for every 5 mintues)
Capacitance at 10 KHz (pF)	157.3	83.7	88.35
Thickness (µm)	0.7	2.7	3.2
Dielectric constant	12.43	32.5	40.67
Breakdown Voltage (V/ µm)	500	>185.2	>156.25

The new procedure thus enables us to increase the fraction of loading with a given nano particle solution. The increase in K value was noted down. The difference in K value is due to the spinning pattern, ozone treatment and shape of the Si wafer. In case of a pie shaped Si wafer, the spinning throughout the wafer is not uniform, since different sides have different length. In order to achieve a uniform spin coating throughout the substrate, polymer printing techniques can be used, in which the growth of the nano composite layer, throughout the wafer can be monitored and controlled easily.

The same experimental procedure can be followed to increase the concentration up to 0.08 % loading or higher, as long as it doesn't reach the percolation threshold.

The scanning electron microscopic images of the capacitors fabricated using the techniques have been shown in figures 6.11 and 6.12. These pictures were taken at an angle of 45°. Hence the tilt compensation was included when determining the thickness of the dielectric.

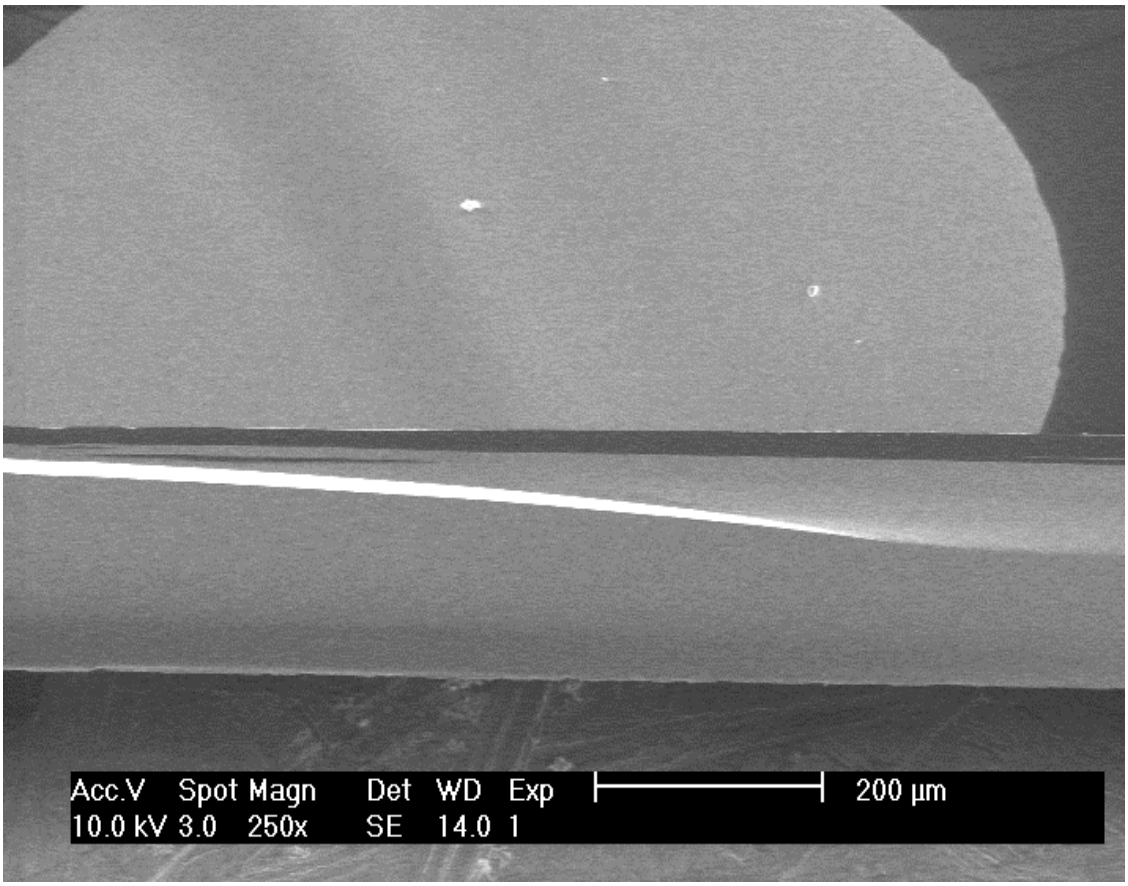

Figure 6.11 SEM image of sample D7

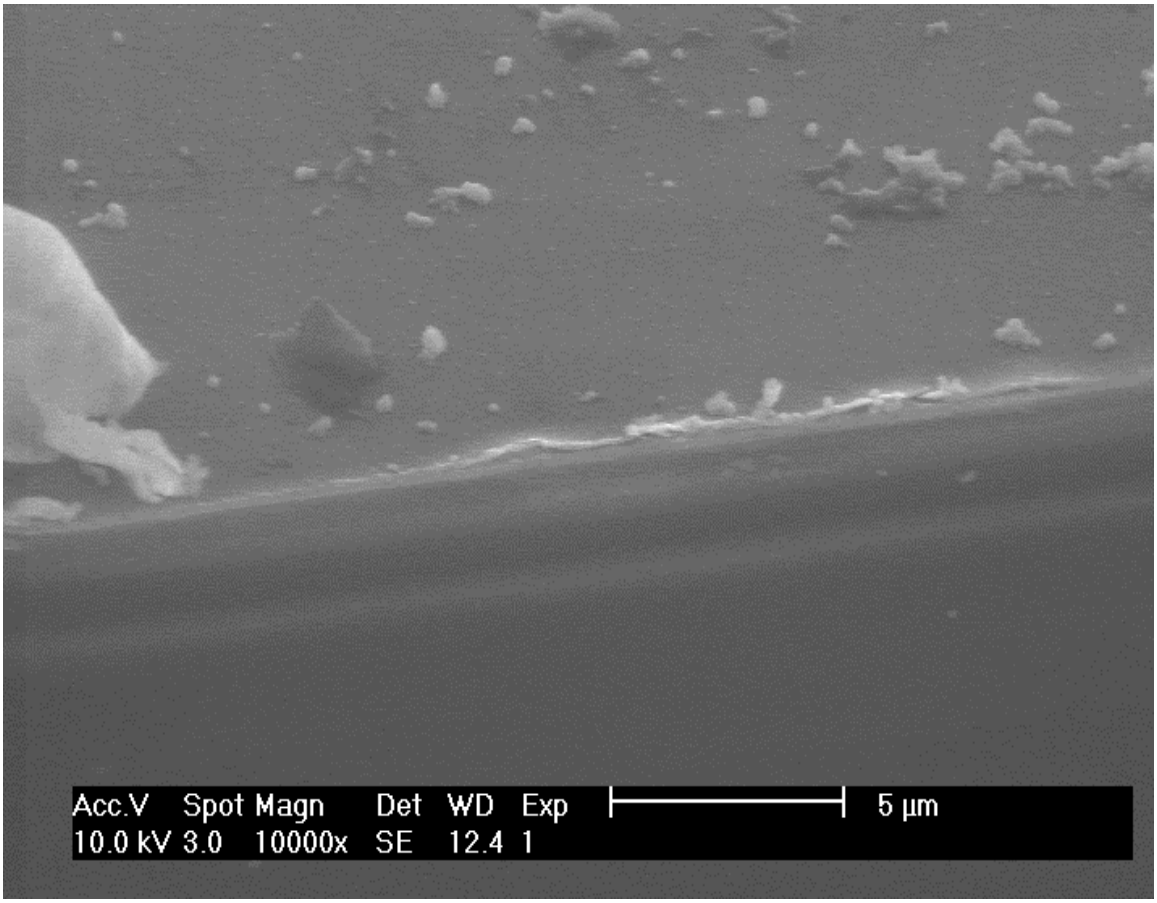

Figure 6.12 SEM image of sample D8

The dark layer sandwiched between two bright layers is the dielectric thin film. Aluminum metal and the silicon wafer are shiny in nature and hence they are shown as bright areas in the image. The thickness of the dielectric varied when different procedures were used for spin coating.

Table 6.4 compares the capacitance density of commercially available capacitors with the results obtained from this work. The table shows that capacitance density achieved with this technique is in range with commercially available values.

Table 6.4 Comparison of commercially available polymer capacitors

Manufacturer	**Hadco**		**3M**	**DuPont**	**UH / IMS**
Trade Name	EmCap	BC2000	C-Ply	HiK	Ag/PVP Nanoparticle Embedded Polymeric Matrix
Dielectric material	Epoxy Resin/Barium Titanate	FR-4	Epoxy Resin/Barium Titanate	Polyimid Core	
Thickness (µm)	100	50	4-25	25	3.2
Capacitance (nF/In^2)	2.1	.5	10-30	1.5	72.57

6.5 Future work

A recent innovation from Intel is about the usage of High K dielectrics as Gate insulators for CMOS devices [19]. Hafnium based dielectrics are used for the same. The dielectric constant of Hafnium oxide is 25. The highest K value obtained from the experiments is 40.67, which is higher than the Hafnium Oxide. Thus these nano

dielectrics can be used to implement the CMOS devices, to obtain high switching characteristics.

The same experiment can be performed with polymers that have high dielectric constant, For example, the polymer, Polyvinylidene difluoride (PVDF) has dielectric constant 12 [12]. PVDF can be included with metal nano fillers to obtain higher K values. The physical properties and chemical properties of the polymer has to be studied before commencing the experiment. For example, PVDF is not soluble in water. But the synthesized nano particles are suspended in water. Hence mixing of PVDF to the nano particle solution would result in a poor nano composite. The nano particles have to be synthesized in a solvent that would dissolve PVDF.

The idea of multilayer film coating can be implemented, in which, the first layer of thin film is made with nano composite solution, and on the top of it, a metal layer has to be deposited, without any mask. Then another layer of nano particle solution has to be gown, on the top of which, there will be metal contacts, made using the mask. Thus the effective device acts as two capacitors, connected in parallel, leading to increased capacitance.

The COMSOL model can be used to determine the break down voltage and other characteristics from the simulation. An effective method to determine the K value of the complete model from the simulation can be designed. The current method involves more complex calculations and thus makes it impossible to determine the K value. When building the model, more conditions can be setup to make the model more realistic.

The same set of experiments has to be repeated again to test if the same K value can be obtained, by following the same procedure. The loading of the nano particles can be increased close to the percolation threshold value and the K value has to be determined. This would provide a comparison between the theoretical and practical values.

CHAPTER 7. CONCLUSION

The nano dielectrics were simulated using the COMSOL and its characteristics such as electrical field, Electric displacement and Electric polarization was studied, in both 2D and 3D models. The dielectric constant of the silver nano particle was calculated using the size dependent Drude-Lorentz model. The theoretical values were obtained using the percolation theory and the effective medium theories. The values were close to each other at low fraction of loadings.

The effective dielectric constant of the nano dielectrics was increased to 40.67 using Silver nano particles dispersed in PVP. An optimized method was designed to increase the K value and also to strengthen the cross link between the nano composite solution and the Si wafer. The LCR characteristics were determined using the LCR meter for range of frequencies 20Hz to 10MHz. The break down characteristics was obtained till 500V.

A new procedure was implemented to increase the fraction of loading of nano particles in the polymer, with very low concentration of nano particles. The fraction of loading was increased up to 0.08% in a polymer matrix, without allowing the agglomeration of nano particles. Devices were fabricated with the same fraction of loading and were tested for their characteristics. A high K dielectric was designed that can be implemented in most of the dielectric applications, by tuning their characteristics to suit the particular application.

REFERENCES

1. J. Lu and C. P.Wong, “Recent advances in high-k nancomposite materials for embedded capacitor application,” IEEE Trans. Dielectr. Electr. Insul.,vol. 15, no. 2, pp. 1322–1328, Oct. 2008.

2. J. Y. Li, L. Zhang, and S. Duchame, “Electric energy density of dielectric nanocomposites,” Appl. Phys. Lett. 90, 132901, 2007.

3. S. K. Saha, “Nanodielectrics with giant permittivity,” Bull. Mater. Sci., Vol. 31, No. 3, June 2008, pp. 473–477.

4. R. Bikky, "Fabrication and characterization of polymer-based high k nano dielectrics for embedded capacitor applications," University of Houston, Houston, 2010.

5. M. Deepak, B. Nacer, B. Abdelhak, "Modelling and simulation of artificial core-shell based nanodielectrics for electrostatic capacitor applications," COMSOL Conference 2011, Boston.

6. A. Kruger, www.iihr.uiowa.edu/~hml/people/kruger/Publications/ChipCenter/micacap.pdf, November’10.

7. www.radio-electronics.com/info/data/capacitor/capacitor_types.php, November 2010.

8. V. Siddharth, “Synthesis of Boron Oxynitride, an Emerging Dielectric, for Use in High Temperature Capacitor Applications,” Electrical Engineering, University of Houston, Houston, 2009.

9. C. J. Kaiser, The Capacitor Handbook, Van Nostrand Reinhold, New York, 1993.

10. R. N. P. Choudhary and P. S. Kumari, Dielectric Materials: Introduction, Research and Applications, Nova Science Publishers, New York, 2009.

11. M. Rabuffi and G. Picci, “Status Quo and Future Prospects for Metallized Polypropylene Energy Storage Capacitors,” IEEE transactions on plasma science, Vol 30, 1939-1942, 2002.

12. Y.Sun Y. Xia, "Shape controleld synthesis of Gold and Silver nano particles",Science 298, 2176 (2002).

13. R. Kirschman, “High-Temperature Electronics”, IEEE press, New York, 1998.

14. A.N. Hammoud, E.D. Baumann, J.T. Myers, and E. Overton, “Electrical Characterization of Glass, Teflon, and Tantalum Capacitors at high temperatures,” Energy Conv. Eng. Conf., 1990, IECEC-90, Proc. Of the 25th Intersociety, Vol. 1, pp.423-427, Aug. 1990.

15. F.P. McCluskey, R. Grzybowski, T. Podlesak, " High Temperature Electronics," CRC press New York, 1997.

16. http://electrochem.cwru.edu/encycl/art-c04-electr-cap.htm.

17. Y. Bai, Z. Y. Cheng, V. Bharti, H. S. Xu and Q. M. Zhang, "High dielectric- constant ceramic-powder polymer composites," Appl. Phys.Lett., Vol. 76, 3804-3806, 2000.

18. Y. Rao, S. Ogitani, P. Kohl and C. P. Wong, "Novel polymer-ceramic nanocomposite based on high dielectric constant epoxy formula for embedded capacitor application," J. Appl. Polym. Sci., Vol.83, 1084-1090, 2002.

19. C. Auth et. al "45nm High-k+ Metal Gate Strain-Enhanced Transistors," Intel Corp., Hillsboro, OR.

20. Y. Rao, C. P. Wong and J. Xu, "Ultra high k polymer metal composite for embedded capacitor application," US Patent 6864306, 2005.

21. J. Wang, Q. Shen, C. Yang and Q. Zhang, "High dielectric constant composite of P(VDF-TrFE) with grafted copper phthalocyanine oligmer," Macromolecules, Vol. 37, 2294-2298, 2004.

22. L. Nicolais and G. Carotenuto, Metal-Polymer Nanocomposites, John Wiley & Sons Inc. Hoboken, New Jersey, 2005.

23. Y. Shen, Y. Lin, M. Li, and C. W. Nan, "High Dielectric Performance of Polymer Composite Films Induced by a Percolating Interparticle Barrier Layer," Adv. Mater, 19, 1418–1422, 2007.

24. G. L. Johnson, Solid State Thesla Coil, www.eece.kce.edu/johnson, Chapter 3-1, 2001.

25. L. G. Chistophorou and L. A. Pinnaduwage, "Basic physics of gaseous dielectrics," IEEE Transactions on Electrical Insulation, Vol 25, No. 1, 55-74, 1990.

26. A. E. Neeves and M.N.Birnboim, "Composite Structure for the enhancement of nonlinear-optical susceptibility," J.Opt Soc. Am. B, Vol 6, No. 4, 787-796, April 1989.

27. L. B Scaffardi and J. O. Tocho, "Size dependence of refractive index of gold nanoparticles," Institute Of Physics Publishing, Nanotechnology, 17, 1309–1315, 2006.

28. U. Kreibig and M. Vollmer, Optical properties of metal clusters, Springer, Springer series in materials science, New York, 1995.

29. R. D. Averitt, D. Sarkar and N. J. Halas, “Plasmon Resonance Shifts of Au-Coated Au2S Nanoshells: Insight into Multicomponent Nanoparticle Growth,” Phys Rev Lett, Vol 78 No 22, 4217-4220, 1997.

30. N. K. Grady, N. J. Halas and P. Nordlander, “Influence of dielectric function properties on the optical response of plasmon resonant metallic nanoparticles,” Chemical Physics Letters 399, 167-171, 2004.

31. W. Zhang, S.H. Brongersma, O. Richard, B. Brijs, R. Palmans, L. Froyen and K. Maex, “Influence of the electron mean free path on the resistivity of thin metal films,” Microelectronic Engineering, 76, 146–152, 2004.

32. V. Myrochnychenko and C. Brosseau, “Finite-element method for calculation of the effective permittivity of random inhomogeneous media,” Physical Review E 71, 016701, 2005.

33. T. C. Choy, Effective medium theory – principles and applications, International series of monographs on Physics, Oxford science publications, New York, 1999.

34. W. M. Merrill, R. E. Diaz, M. C. Squires and N. G. Alexopoulos, “Effective Medium Theories for Artificial Materials Composed of Multiple Sizes of Spherical Inclusions in a Host Continuum,” IEEE Transactions on antennas and propagation, 47, No. 1, 142-148, 1999.

35. C. W. Nan, Y. Shen and J. Ma, “Physical properties of composites near percolation,” Annu. Rev. Mater. Res, 40, 3.1–3.21, 2010.

36. G. Grimmett, Percolation, Springer link, New York, 1991.

37. D. W. Pepper and J. C. Heinrich, The finite element method: Basic concepts and applications, Hemisphere publishing corporation, USA, 1992.

38. O. C. Zienkiewicz, R. L. Taylor and J. Z. Zhu, The finite element method: Its basics and fundamentals, Elsevier Butterworth-Heinemann, Burlington, 2005.

39. G.R. Liu and S. S. Quek, The finite element method: A practical course, Elsevier Butterworth-Heinemann, Burlington, 2003.

40. G. Fren, “Controlled nucleation for the regulation of the particle size in monodisperse gold suspensions,” Nature: Phys. Sci. 241, 20-22, 1973.

41. Y. Kobayashi, A. Kosuge and M. Konno, “Fabrication of high concentration barium titanate/polyvinylpyrrolidone nano-composite thin films and their dielectric properties,” Applied Surface Science, 255, 2723–2729, 2008.

42. R. Dorf “Introduction to Electric circuits” ISBN 0-471-38689-8.